OPTIMAL PROCEDURE FOR ENERGY MANAGEMENT IN SOLUTION MINING OF SALT DOME CAVERNS

By

JAMES HARRY NORTON

Bachelor of Science
Oklahoma State University
Stillwater, Oklahoma
1967

Master of Science
Oklahoma State University
Stillwater, Oklahoma
1971

Submitted to the Faculty of the Graduate College
of the Oklahoma State University
in partial fulfillment of the requirements
for the Degree of
DOCTOR OF PHILOSOPHY
July, 1978

OPTIMAL PROCEDURE FOR ENERGY MANAGEMENT

IN SOLUTION MINING OF

SALT DOME CAVERNS

Thesis Approved:

James E. Shamblen
Thesis Adviser

M. Palmer Terrell

James E Bose

Joe H. Mize

Donald W. Grace

Norman N Durham
Dean of the Graduate College

ACKNOWLEDGMENTS

I wish to express my appreciation and gratitude to my major adviser, Dr. James Shamblin, for his guidance and assistance throughout this research. I have enjoyed his classroom manner while teaching operations research techniques. To Dr. Joe Mize, I express my sincere thanks for his instruction in discrete and continuous system simulation and general large-scale system modelling. Special appreciation is also expressed to three other advisory committee members, Dr. M. Palmer Terrell, Dr. James E. Bose, and Dr. Donald W. Grace, whose instruction in classical optimization, search techniques and computer-aided solution methods has been used for this research.

During the writing of this dissertation I have been employed by Fenix & Scisson, Inc., a worldwide constructor of underground storage caverns. I wish to express my thanks to the management who have encouraged and supported my research and to Jesse Wyrick who taught me the fundamentals of solution mining.

Sincere appreciation is given to my family and friends who continually encouraged me throughout this endeavor. Finally, thank you Linda for your understanding for this part-time husband.

TABLE OF CONTENTS

LIST OF TABLES

LIST OF FIGURES

Figure Page

LIST OF SYMBOLS

Symbol	Definition	Units
$A_{i,j}$	cell cross sectional flow area at Section i of Cell J	ft^2
C	factor whose value depends upon the fluid	
C_i	loss constant for a particular valve or fitting	
D_I	internal diameter of large suspended casing	in
D_O	outside diameter of large suspended casing	in
d	inside diameter of pipe	ft
d_i	inside pipe diameter or equivalent diameter of pipe annulus between Points i and i + 1	in
d_I	internal diameter of small suspended casing	in
d_O	outside diameter of small suspended casing	in
$E_{\Delta T}$	energy consumed during time interval ΔT at power level P_r	kw-hrs
f	friction factor	
g_c	dimensional constant, 32.174	$\frac{lb_m ft}{lb_f sec^2}$
g_o	acceleration due to gravity, 32.174	ft/sec^2
h_L	head loss due to pipe friction and flow through fittings	ft
h_8	height of fluid above inlet to brine holding tank	ft
K_1	constant for converting to correct units	

Symbol	Defintition	Units
L_{fvi}	equivalent length of pipe corresponding to fittings, valves, etc., between Points i and i + 1	ft
L_e	equivalent length of pipe corresponding to a particular fitting or valve	ft
L_i	length of pipe between Points i and i + 1	ft
P	pump pressure	lb_f/in^2
P_i	pressure at Point i, or fluid pressure at Section i of a pipe or cavern cell	lb_f/ft^2
$P_{i,j}$	cell pressure at Section i of Cell j	lb_f/in^2
P_r	hydraulic power required to maintain flow at pump pressure, P_1, and flow rate, Q_4, or hydraulic power required to maintain flow at pump pressure, P, and flow rate, Q	kw
Q	pump flow rate	gal/min
Q_i	flow rate between Points i and i + 1	gal/min
$Q_{i,j}$	cell flow rate through Section i of Cell j	gal/min
Q_1	flow rate at Point 1	gal/min
Q_5	flow rate at Point 5	gal/min
R_{cap}	spherical cap ratio of output volume to input volume	
$\hat{R}_i$	average cell radius of Cell j	ft
$R_{i,j}$	cell radius at Section i of Cell j	ft
R_j	cell ratio of output volume to input volume of Cell j	
s.g.	specific gravity of fluid	

Symbol	Definition	Units
$sg_{i,j}$	cell fluid specific gravity at Point i of Cell j	
$\hat{sg}_j$	average specific gravity of Cell j	
sg_1	specific gravity of fluid at Point 1	
sg_5	specific gravity of fluid at Point 5	
V	average velocity of fluid	ft/sec
$V_{i,j}$	cell fluid velocity at Section i of Cell j	ft/sec
V_4	fluid velocity at Point 4	ft/sec
V_5	fluid velocity at Point 5	ft/sec
v_i	fluid velocity at Section i of a pipe or cavern cell	ft/sec
Z_i	elevation at Point i, or elevation at Section i	ft
$Z_{i,j}$	elevation at Section i of Cell j	ft
ΔT	time interval	hrs
ρ	mass density of fluid	lb_m/ft^3

CHAPTER I

INTRODUCTION

The major objective of this research is to develop a guideline for energy awareness and conservation for the solution mining industry. This verbal objective will be translated into a mathematical formulation using value or multiobjective theory and solved using fundamental optimization. Besides the technique developed for this research, hard numbers are calculated and presented as optimal solutions and managerial operating ranges for controlling the variable under consideration for a specific project.

Solution mining activities include the creation of large caverns in salt deposits by exposing the salt in a drilled hole, then injecting raw (fresh or low salinity) water into the hole, allowing time for the salt to dissolve, and removing the resulting brine. The activity may be for the purpose of producing brine for chemical feedstock or for the purpose of underground storage of certain raw materials and chemical products.

The use of solution mined salt caverns has become one of the most popular methods of storing large volumes of hydrocarbons. Since 1950, advances in engineering and construction techniques and experience in solution mining have made possible a more diversified use of salt for underground storage.

Salt exhibits a unique combination of characteristics, making it the ideal rock for cavern construction. It is impervious to many liquids and gases, has a compressive strength comparable to concrete, moves plastically to seal fractures or voids, and can be easily mined by dissolution in water. Construction is feasible wherever salt, leaching water and conditions for brine disposal coexist in adequate quantity and form.

Construction Techniques

Two basic construction techniques--direct circulation and reverse circulation--are normally used. Direct circulation involves injection of water near the bottom of the drilled hole and withdrawal of brine at a higher point. Figure 1 illustrates this concept. A concentric string of casing is installed in the drilled hole as shown in the figure and is used for fresh water injection and brine withdrawal.

For reverse circulation water is injected down the casing annulus, entering near the top of the cavern, displacing brine into the casing at the bottom of the cavern.

Blanket Material

Blanket material is any substance (gas, propane, butane, diesel oil, crude oil) lighter than water, which occupies the space in the topmost interval of the cavern. A major function of the blanket is to prevent the cavern roof from migrating upward during construction.

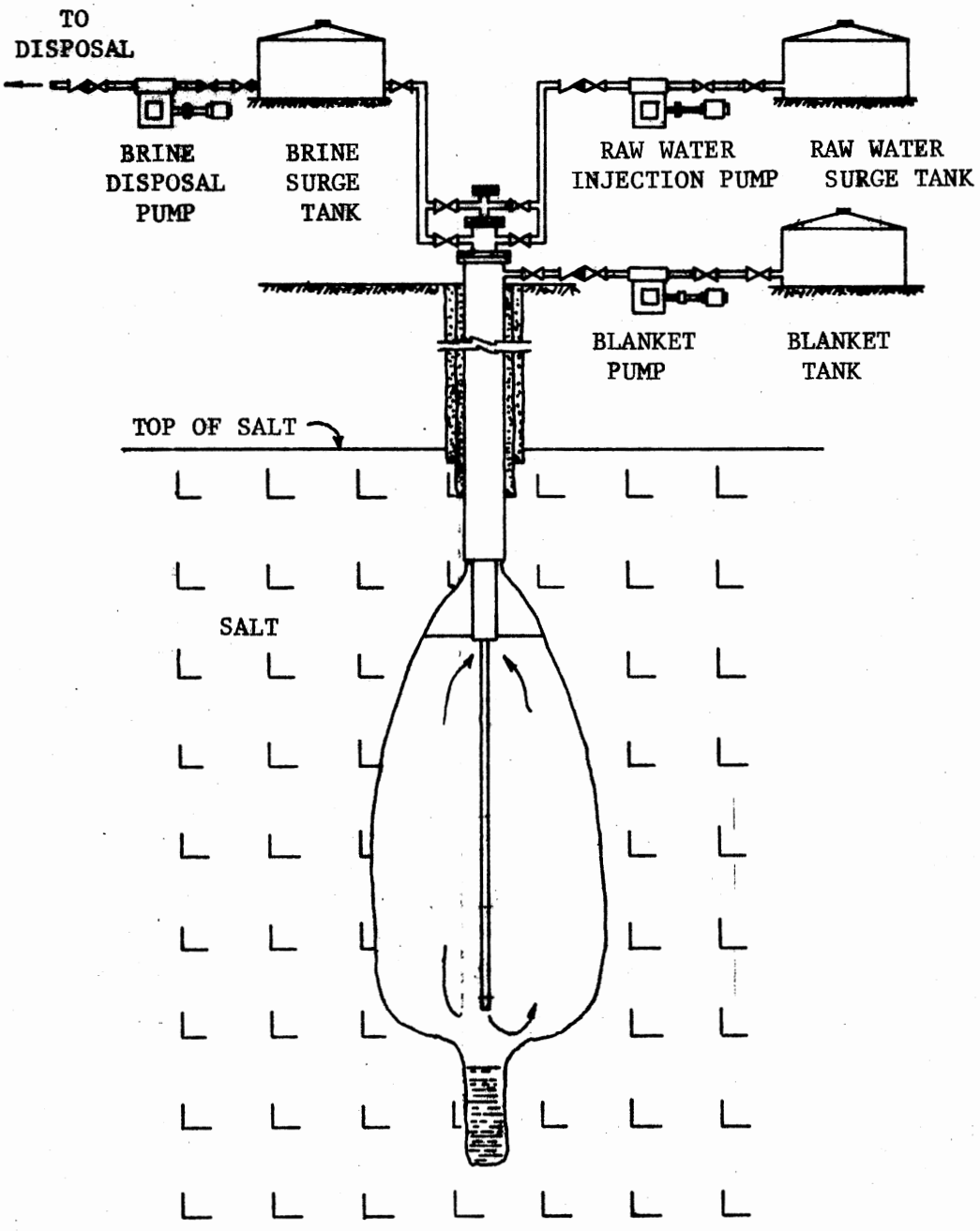

Figure 1. Cavern Construction Using Direct Circulation

The Problem

For all solution mining projects water must be pumped from a water source to the cavern site, then circulated underground and back to the surface where the resulting brine is pumped to a disposal facility. Energy is consumed due to pumping during the cavern construction process called leaching. For 100-percent efficient leaching, defined as the resulting brine being a 100-percent saturated solution, approximately six barrels of water must be pumped underground to create one barrel of cavern space.

The number of new construction projects to create underground storage space for future use is uncertain, but a dramatic increase is expected in cavern construction in the next five years. In addition to construction by private enterprise, Congress has authorized approximately one billion barrels of storage space to be filled with crude oil as part of a national strategic storage plan. A large portion of this space will result from new construction. In comparison, at the present time there is about 350 million barrels of petroleum products storage in service which has taken roughly 20 years to construct.

The conservation of energy is of national importance, so are measures effecting energy conservation or the reduction of energy waste. For example, the Energy Policy and Conservation Act (EPCA) of 1975 has made funds available through the Federal Energy Administration for states to develop and implement energy conservation plans. A goal of these plans is to achieve a five percent energy savings by 1980 through mandatory and non-mandatory programs (1).

If the large cavern construction programs anticipated for the future are required to adhere to state or federal energy conservation

guidelines, then a vehicle is needed to study each specific project in order to prescribe practical conservation measures. In this research the vehicle is developed, and its use is illustrated for a realistic storage project consisting of medium-size (approximately four million barrels) caverns.

Previous work particularly relevant to this research includes efforts made and reported in America, France, and Germany. In America basic laboratory experimentation resulted in a computer program to predict cavern growth and shape through time for given input data. Also a computer program to simulate the growth of a cavern was developed in France and tested at a gas storage operation. Investigators in Germany report the development and use of a three-dimensional computer model for predicting cavern growth rate and shape. Chapter II will discuss this literature in more detail.

The work performed in Europe and in some parts of the United States is carried out in salt deposits that are often interbedded with insoluble layers of material. A salt dome is a geological structure thought by some investigators to have been extruded upward from a mother salt located at great depths. This type of salt deposit is more nearly homogeneous than the bedded deposits but may contain low percentages of insolubles such as sand. This research considers only caverns constructed in homogeneous salt domes that may include construction of a special sump to collect insolubles.

Research Objective

The objective of this research is to determine a realistic plan of energy conservation to be used in constructing medium-size salt dome

storage caverns in which 1) the total energy consumed is minimized and 2) the construction time is minimized. In addition a minimum of five percent savings in total energy consumption is to be realized when compared to a conventional construction technique that uses total pumping capacity throughout the construction phase. The rate at which brine is produced from the cavern is a measurable and controllable construction variable and is the subject of investigation for this research. For a given physical construction system with only the flow rate being variable the following conflict in objectives exists. Total energy consumed is minimized as the flow rate is decreased, but the construction time is minimized as the flow rate is increased. Therefore, a plan is sought that will specify the range of values that the produced brine flow rate may assume in order to meet the research objective.

A realistic plan is one that can be implemented under actual field construction conditions. For example, the plan developed from a mathematical investigation might specify that the flow rate should be controlled not only continuously through time but also with a continuous degree of control at any particular time. To accomplish this objective an automatically-controlled pumping facility might be used whose flow rate can be set at any desired point between zero and maximum flow. However, this research will be tailored for use in a facility operated by field personnel with a finite number of pumping units not having infinite flow control.

Research Methodology

The research was performed in eight separate phases as illustrated in Figure 2.

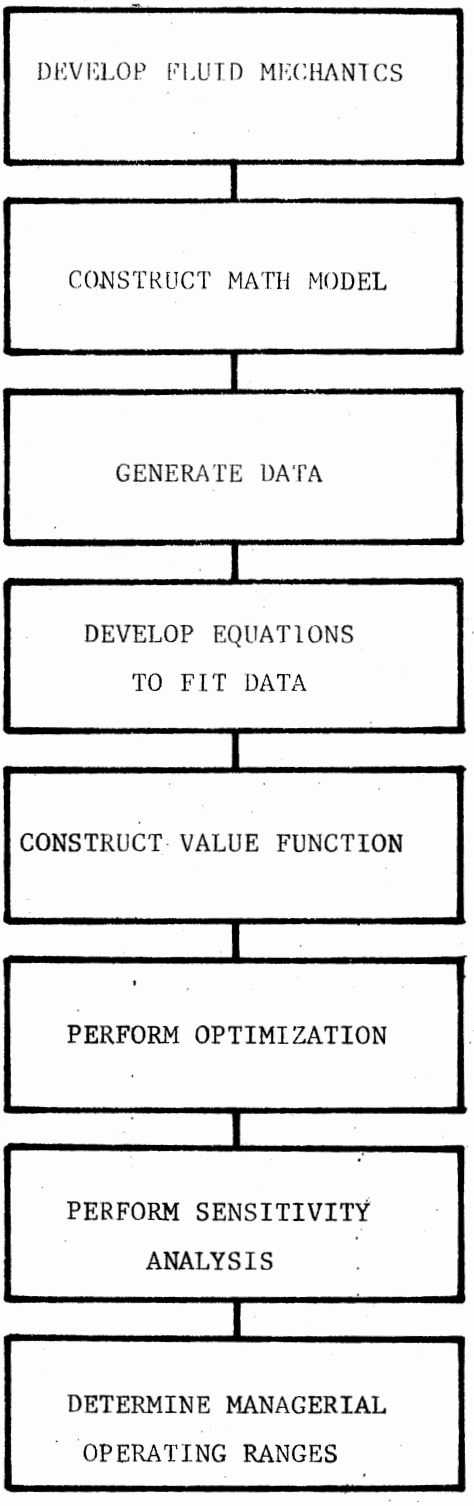

Figure 2. Flow Chart Showing Research Methodology

Construction of the fluid mechanics theory as Phase 1 was most time consuming. This phase included 1) determination of the physical elements used to model a typical cavern construction system and 2) development of the fluid mechanics to describe energy consumption during a solution mining activity. Briefly, the elements modelled include a surface piping system, the storage cavern well casings and the cavern itself. Chapter III contains a detailed description and illustration of the general system.

Three different principles of fluid mechanics were considered before a final decision was made on how to express cavern construction in terms of energy consumption. First, the general energy equation was discarded because of the lack of published information on thermodynamic properties such as internal energy and enthalpy of various brine saturations. Next, the conservation of momentum was studied, but was also discarded because equations describing system forces resulted in more unknowns than equations. Finally, the conservation of matter leading to the Bernoulli equation was found to be acceptable for the purpose of this research. The general fluid mechanics theory is the subject of Chapter III.

Phase 2 involved construction of the mathematical system model in which fluid mechanics equations were written for each physical system element. The cavern was modelled as a series of horizontal disc shaped cells. A computer program was then developed integrating the fluid mechanics with an existing research program written to describe cavern growth and the salt dissolution process. The mathematical model of the system is given in Chapter IV.

In Phase 3 the computer program was used to generate data concerning construction times and energy consumption for both sump construction and cavern construction. A set of realistic values was assigned to system input variables thus defining a test construction system. Ten simulated construction activities were run each for a 400,000 barrel sump and a four million barrel cavern. For the sump and cavern the runs were made for constant flow rates between 300 gallons per minute (gpm) and 3,000 gpm in increments of 300 gpm.

In Phase 4 the data generated from the computer runs were fitted resulting in mathematical equations expressing sump and cavern construction times and total energy consumed for sump and cavern construction as functions of the produced brine flow rate. Phase 5 involved using these relationships to formulate value functions for sump and cavern construction. A value function is the mathematical expression of the research objective.

In Phase 6 optimal values were found for each of the value functions. A sensitivity analysis was performed for each value function in Phase 7, and was used in Phase 8 to determine the operating range for the produced brine flow rate that will maintain the value function within a predescribed deviation from its optimal value. The operating range is called the managerial operating range. The work in Phases 3 through 8 is contained in Chapter V. Since the techniques used were somewhat sensitive to roundoff error, numerical values involving many significant figures were published as calculated.

Results of Research

To the knowledge of the writer this study represents the first research and application model of its kind and completeness made available for the general use of the solution mining industry. This research complements and extends the experimental laboratory work and resulting computer program published by Saberian (2) describing cavern growth, cavern shape, and the general dissolution process.

Using this research the following capabilities are available for general use:

1. An actual construction project with its associated surface piping, wellhead and well casing may be modelled.
2. By supplying values for input parameters energy consumption may be studied for various test cases.
3. For a given system model the relationship between produced brine flow rate and energy savings can be determined.
4. When the relative importance of minimizing construction time and minimizing total energy consumed can be expressed, then the optimal produced brine flow rate to accomplish this objective for a given system can be determined.
5. When an allowable deviation is permitted from the optimal value of the objective, then a corresponding range of operation for the produced brine flow rate can be determined.

CHAPTER II

LITERATURE REVIEW

This research deals with an established sector of industry in which experience, technical knowledge, and research are not necessarily reported or made available for public use. Information that is available may be found in trade journals or proceedings of various society meetings. For example, a series of four "Symposiums on Salt" have been held generally every fourth year beginning in 1963 with the most recent one held in 1974. The publications (3) resulting from these meetings include field case studies and laboratory and theoretical research pertaining to solution mining activities.

A second source of literature is published under the control of the Solution Mining Research Institute, Inc. (SMRI) composed of individuals and industrial companies and organized in 1965 to promote activities concerned with producing brine from salt deposits. SMRI funds theoretical and laboratory research conducted at the University of Texas at Austin. Results of the research are available to members and is sometimes made public.

Information dealing with solution mining is also developed by private companies as a result of field experience or privately funded research. This is often proprietory and not available for public use.

To the knowledge of this researcher there are no publications quantitatively relating cavern construction and energy input. There has been published research concerning cavern formation.

Jessen (4) discusses the solution mechanisms involved during the brining of salt deposits. Remson, Dommers, and Jessen (5) discuss techniques which provide means of obtaining various shaped cavities.

At least four numerical analysis programs have been written to simulate the creation of a cavern in salt by solution mining. Pottier and Esteve (6) constructed and used a numerical model to simulate cavern development in bedded salt intermingled with layers of insoluble clay and anhydrite. Figure 3 compares the results of actual cavern construction near Lyon, France with simulation results. Pottier and Esteve reported a very good fit between the simulation results and field measurements.

A three-dimensional computer model developed by researchers in Germany is reported to predict the concentration of brine, the increase in cavern space, and the cavern shape for a leaching process where the depth of the leaching casings and the blanket level are not held constant (7). The model has been tested in bedded salt with layers of impervious material intermingled in the salt body. An additional and important factor concerning this model is its ability to simulate cavern construction parameters when the drilled hole is not completely vertical.

Snow and Chang studied the problem of cavern growth due to the long term exposure of a drilled hole to very small water feed rates (8).

The document most relevant to this research is entitled "Numerical Simulation of Development of Solution-Mined Salt Cavities" (2) written by Dr. Ahmad Saberian while a graduate student at the University of

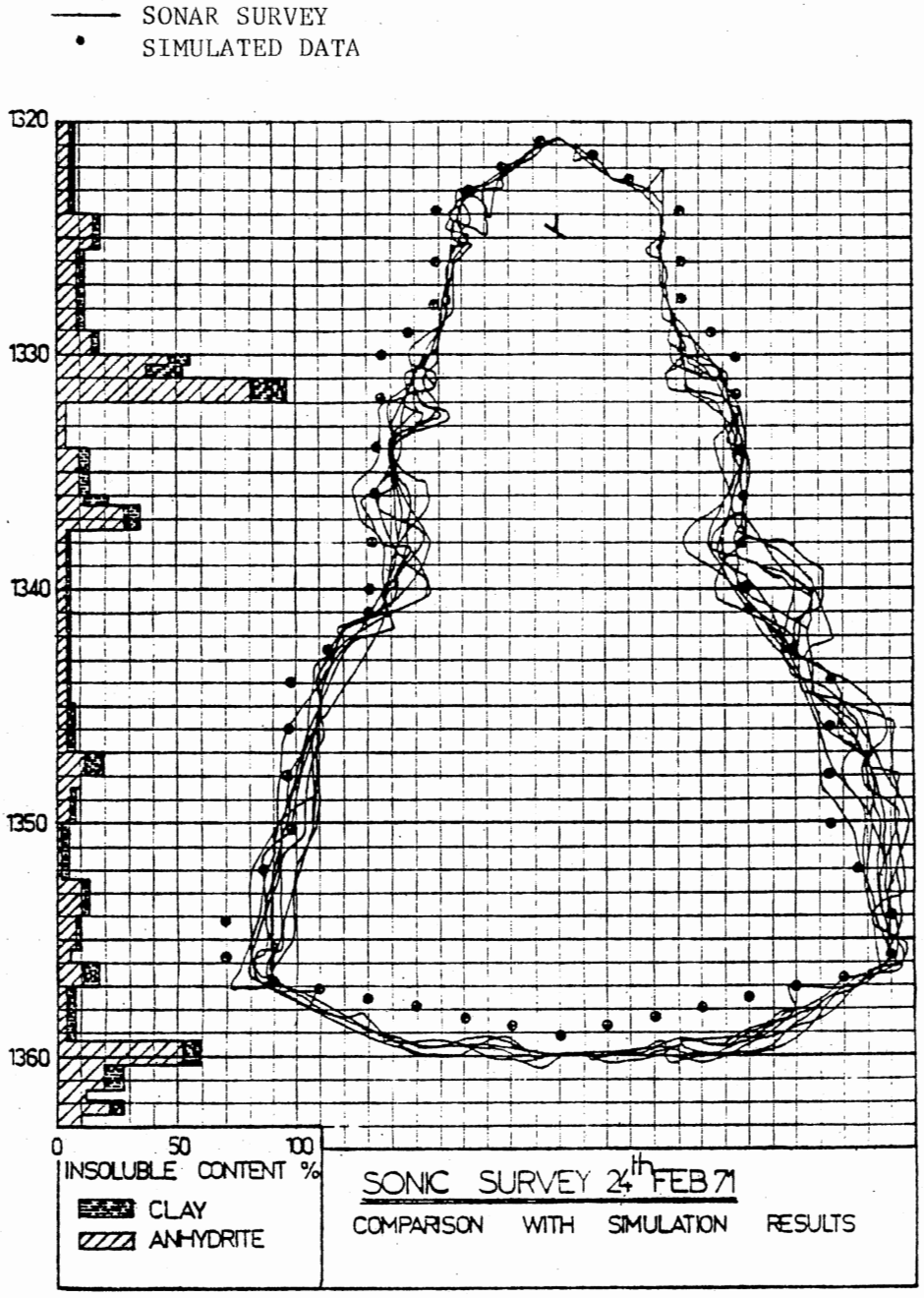

Figure 3. Cavern Construction in Bedded Salt Deposit (6)

Texas at Austin. The document (which was Saberian's doctoral thesis) is a progress report on research supported by SMRI and discusses the mechanism of salt dissolution and includes the mathematics involved in cavern growth.

Saberian's publication presents the results of a great deal of laboratory investigation leading to the formulation of salt dissolution process equations. The resulting FORTRAN computer simulation code is given in an appendix of his report. To verify the computer program Saberian simulated and reported on the dissolution process for two caverns which had actually been constructed (2).

In order to insure correct use of the simulation code this researcher formulated and reran one of Saberian's test cases and obtained duplicate results. Figure 4 shows the results of comparing Saberian's simulation prediction with an actual cavern constructed in dome salt. The figure illustrates excellent agreement in the predicted and actual cavern shapes.

In addition to cavern shape, Saberian's simulation program calculates values for the salinity of the produced brine, the cavern size, and various other parameters.

The intent of this research was not to attempt to improve upon the accuracty of Saberian's program, but to integrate his work with a procedure to determine energy usage during cavern construction.

No previously published work was found concerning application of multiobjective functions to the solution of problems in the solution mining industry, although many references were given a cursory review that dealt with problems related to other disciplines. In general, a wide variety of case studies are available in trade journals and

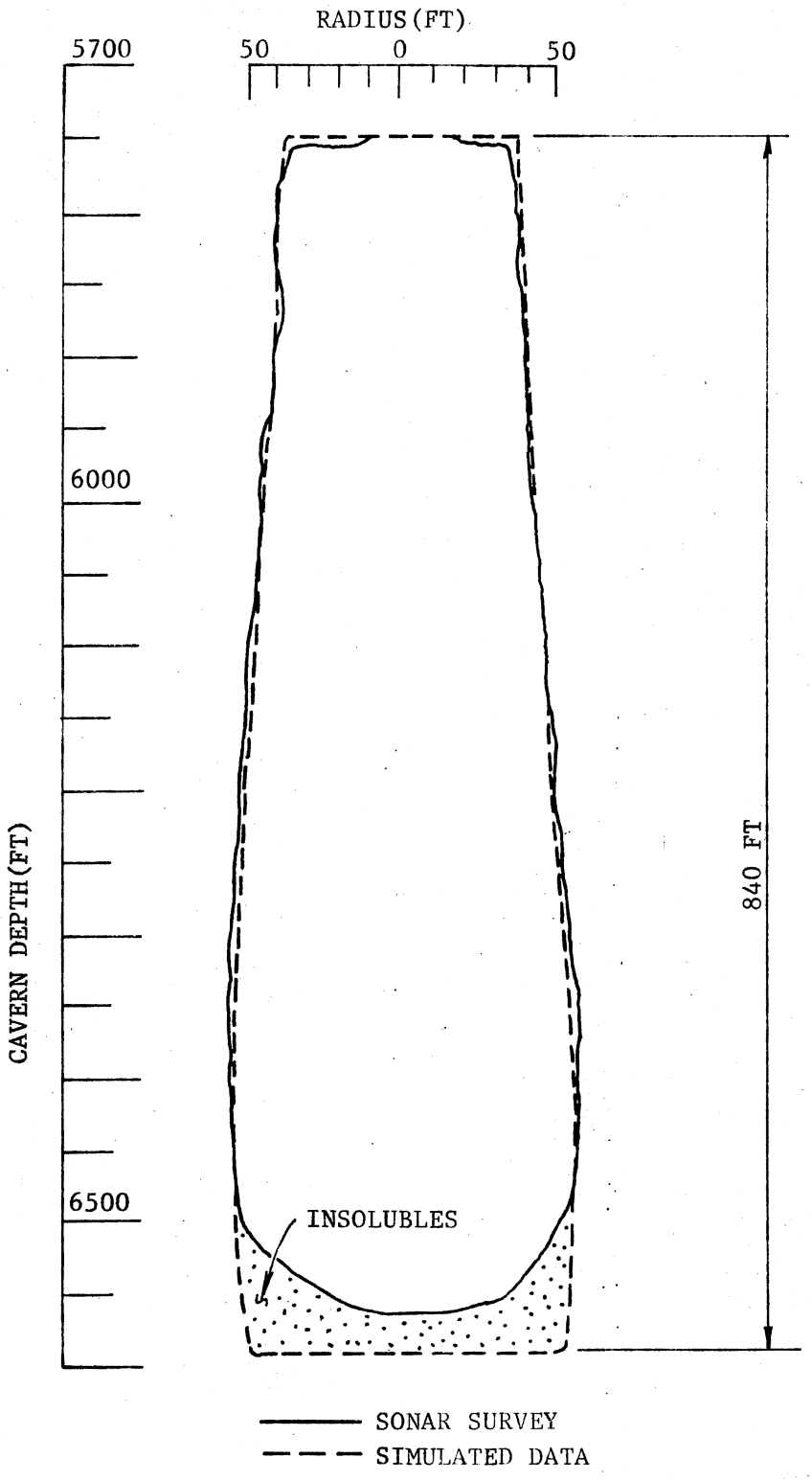

Figure 4. Cavern Construction in Dome Salt (2)

published articles and papers in which multifactor functions are formulated to study specific problems. Interested readers could review literature categorized as value theory, goal programming, utility theory and multifactor objective theory.

Fluid mechanics theory relating to the conservation of energy, momentum, and matter can be found in many texts. Theory used in this research was based on derivations by Brenkert (9).

For this research, the general formulation for expressing an objective composed of factors of dissimilar entities is given by Gottfried and Weisman (10). They utilize an approach known as value theory to express a multifactor objective function in mathematical terms. The resulting value function is formulated as

$$V = \sum_{i=1}^{n} w_i V_i$$

where V is the total value of the function; w_i is a weighting factor used to express the relative importance of entity i; V_i is the value of entity i. Each V_i is a function of one or more of the problem variables resulting in

$$V = \sum_{i=1}^{n} w_i f_i (x_1, x_2, \ldots, x_m).$$

The value of each entity is scaled such that all possible values for a particular entity lie between 0 and 1.

Abouel-Nour (11) presents a sensitivity analysis for many models composed of 1) two different standard curves, 2) three different standard curves. The standard curves he reviewed were the straight line,

circle, ellipse, parabola, rectangular hyperbola, Gaussian and catenary. For each combination of these increasing and decreasing curves he first found an optimal value expression Y_o as function of the problem variables, then associated an error term w with Y_o such that $Y_w = wY_o$. The error term represents a deviation from the optimal solution. Next a general sensitivity expression was formed as

$$\frac{Y_w}{|Y_o|},$$

and by setting a percentage allowable deviation from the optimal solution, a range on the decision variable called the managerial operating range was determined.

Specifically pages 64-70 of Abouel-Nour's work applies to this research except for his determination of the optimal solution of the resulting cubic value functions. Newman (12) on pages 197-199 gives the solution procedure used to find the roots of the cubic equations and in determination of the managerial operating ranges.

A procedure for the development of a general managerial operating range is given by Shamblin and Stevens (13) in Chapter 9 and was used for this research.

CHAPTER III

FLUID MECHANICS

This chapter develops the fluid mechanics necessary to express solution mining in terms of energy consumption. The fluid mechanics will be translated into a math model for a typical sump and cavern construction system in the following chapter.

Typical Cavern Construction Layout

A simplified typical piping schematic for cavern construction using reverse circulation is shown in Figure 5. Computerized calculations were made to determine the energy required to pump leach water from the injection pumps to the wellhead and circulate it through the cavern and back to the surface where the resulting brine is piped to a holding tank. This flow path is divided into seven segments between Points 1 and 8 as illustrated in the figure.

Segment 1-2 extends from the point where the injection pump discharges are manifolded into a single pipeline to a point near the wellhead where transition is made between the pipeline and the wellhead piping. The number of injection pumps used depends on several factors which include the flow rate requirement and the pumping system flexibility desired. The pumps are manifolded together to supply a combined flow rate and pressure at Point 1.

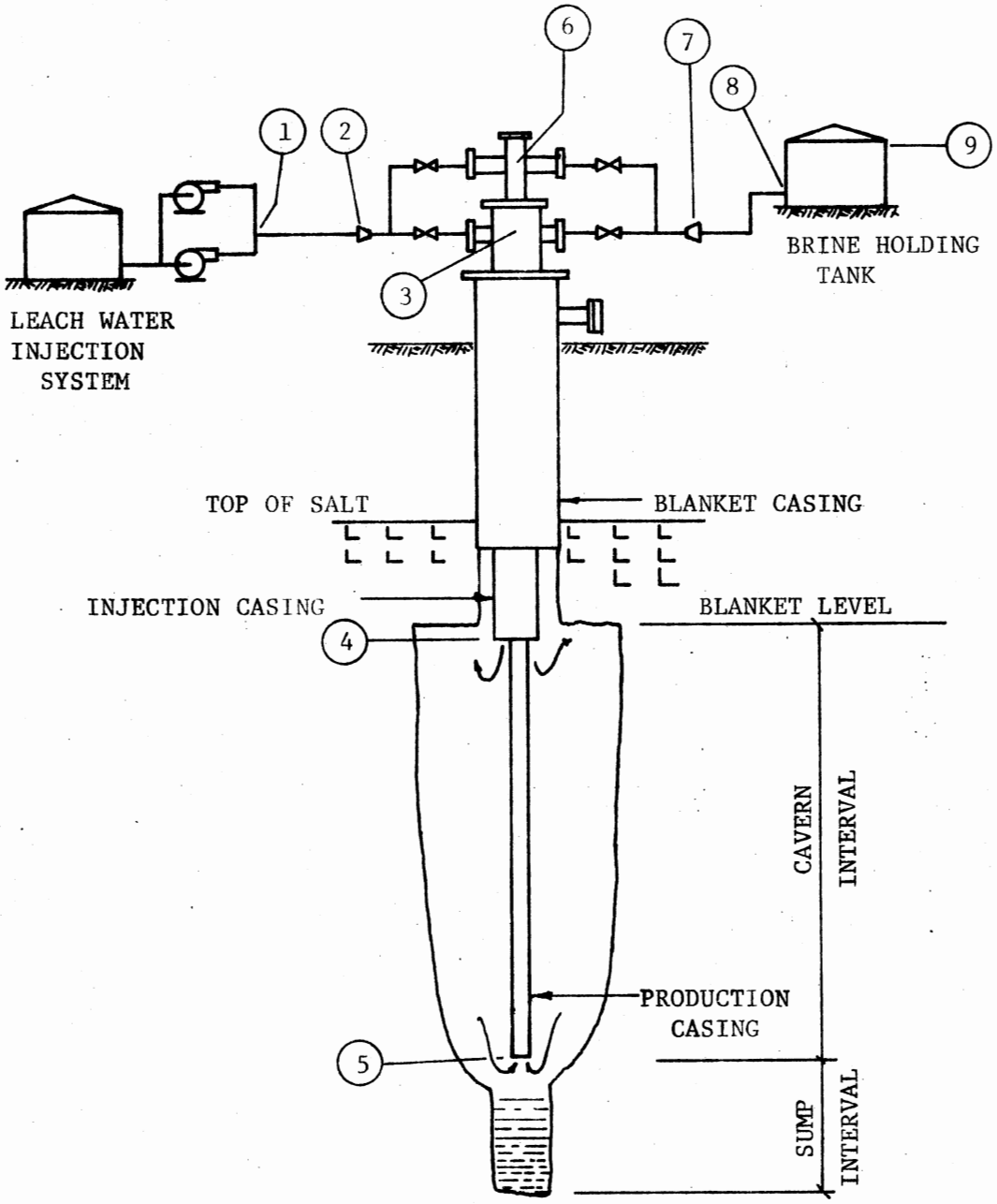

Figure 5. Typical Cavern Construction Piping System

In actual construction the pipeline joining Points 1 and 2 may be larger in diameter than the wellhead piping and valving. Also the wellhead piping and valving is commonly arranged as shown in Figure 5 so that either direct or reverse circulation may be used. Point 2 is selected at the reduction in pipeline diameter at the wellhead and/or before the piping is split to accomodate either direct or reverse circulation. Segment 2-3 includes wellhead valving and piping for the leach water injection system.

Segment 3-4 is the injection casing. Point 3 is located where the wellhead piping intersects the injection casing, and Point 4 is at the lower end of the casing and is always denoted as the inlet to the cavern. For direct circulation the injection casing is the smallest diameter casing suspended in the cavern, and for reverse circulation the injection casing is the largest suspended casing in the cavern.

Point 5 is at the lower end of the production casing and is always the brine outlet from the cavern. Segment 4-5 therefore represents the beginning and end respectively of the flow path in the cavern. Segment 5-6 is the brine production casing, and Point 6 is located at the intersection of the brine production casing and the associated wellhead piping.

Segment 6-7 includes the brine wellhead piping and valving. Segment 7-8 is the pipeline from the wellhead to the brine holding tank. Point 7 is located downstream of the wellhead at the point where the diameter of the piping has been increased to the pipeline diameter. Point 8 is at the point where the pipeline connects to the tank, and Point 9 is the level of fluid in the brine holding tank.

Fluid Mechanics

The fluid mechanics used for analysis of the cavern construction system are based on a form of the Euler equation. A development of the theory, including the assumptions necessary for its use, is presented by Brenkert (9) in Chapter III, V and VI.

The fluid mechanics will be used to determine the pumping pressure required at a given flow rate to circulate fluid through the system. Energy consumption will then be calculated by the following formulae:

$$P_r = \frac{PQ}{2298.5} \tag{3-1}$$

$$E_{\Delta T} = P_r \, \Delta T \tag{3-2}$$

where:

P_r = hydraulic power required to maintain flow at pump pressure P and flow rate Q, kw

P = pump pressure, lb_f/in^2

Q = pump flow rate, gal/min

$E_{\Delta T}$ = energy consumed during time interval ΔT at power level P_r, kw-hrs

In Equation 3-1 the pump pressure must be determined in order to calculate power. To obtain the pump pressure at Point 1 in Figure 5, the calculation process will begin at Point 8 (where known conditions exist) of the same figure and procede backwards through the system to Point 1.

The theory will now be applied to pipe flow and cavern flow.

Pipe Flow

Figure 6 illustrates a portion of pipe with one end elevated above the other. Applying the theory for an incompressible fluid to flow in the pipe between Sections 1 and 2 results in the following expression,

$$\frac{V_2^2 - V_1^2}{2} + g_o (Z_2 - Z_1) + \frac{(P_2 - P_1)g_c}{\rho} + g_o h_L = 0. \qquad (3\text{-}3)$$

where:

V_i = uniform cross sectional velocity at Section i, ft/sec

Z_i = elevation at Section i, ft

P_i = pressure at Section i , lb_f/ft^2

ρ = fluid mass density, lb_m/ft^3

h_L = head loss caused by pipe friction and flow through fittings, valves, wellheads, etc., ft

g_o = gravitational acceleration, 32.174 ft/sec^2

g_c = dimensional constant, 32.174 $lb_m.ft/lb_f.sec^2$

Since the velocity is constant, $V_1 = V_2$ and Equation 3-3 is rewritten as

$$\Delta P = P_1 - P_2 = \rho\frac{g_o}{g_c}(Z_2 - Z_1) + \rho\frac{g_o}{g_c}h_L. \qquad (3\text{-}4)$$

Friction Losses

An equation to directly calculate pipe friction losses is proposed and used in this research. A form of the Hazen-Williams equation used for pipeline flow is given below.

$$\Delta P_f = K_1\left[\frac{Q}{C\ d^{2.63}}\right]^{1.85} (s.g.)\ L \qquad (3\text{-}5)$$

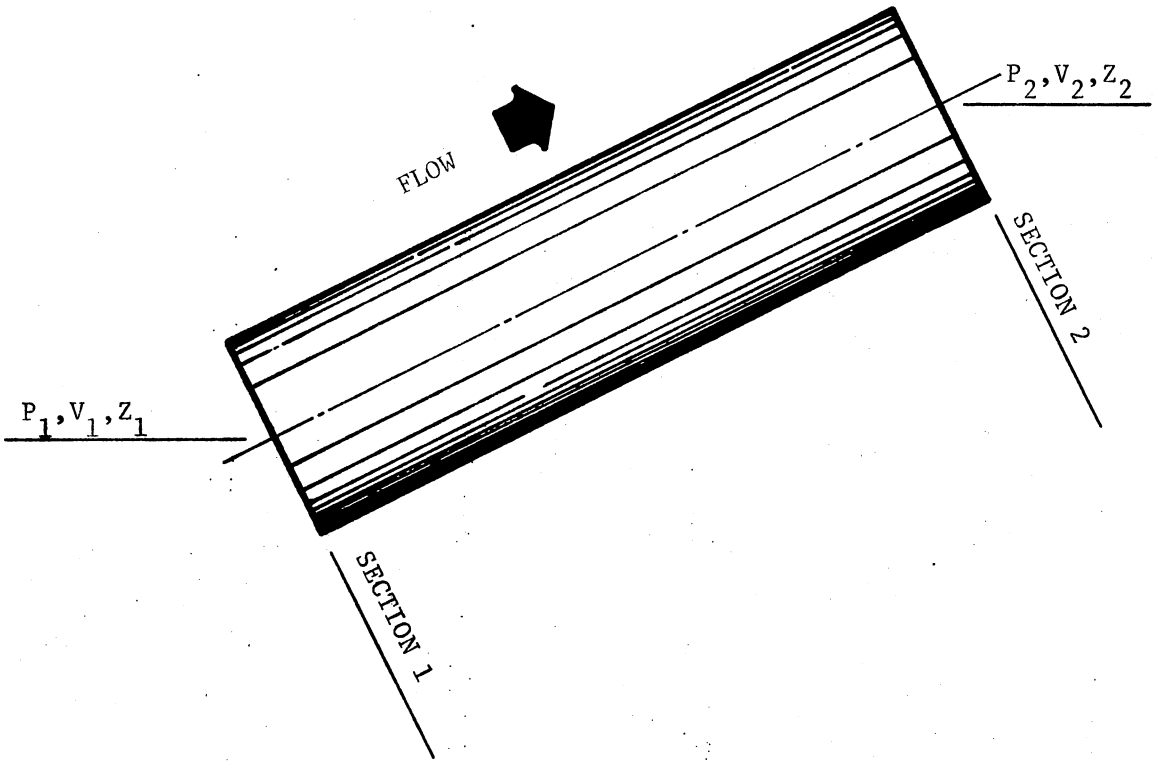

Figure 6. Typical Section of Pipe

where:

ΔP_f = pressure drop due to friction, lb_f/ft^2

K_1 = constant for converting to correct units

Q = flow rate, gal/min

C = factor whose value depends upon the fluid and pipe wall conditions (125 for water, 110 for saturated brine)

d = pipe diameter or equivalent annular diameter, in

s.g. = specific gravity of fluid

L = length of pipe, ft

The form of the Hazen-Williams equation used with this research is given below:

$$\Delta P_f = 645.8\ L\left[\frac{Q}{C\ d^{2.63}}\right]^{1.85} (s.g.). \qquad (3\text{-}6)$$

Other Losses

Other pressure losses occur in piping systems that are not due to friction but are caused by the various fittings and valves used. The fittings and valves for a given line size may be converted to an equivalent length of pipe of the same size and summed as shown in Equation 3-7.

$$L_{fv} = \Sigma L_e \qquad (3\text{-}7)$$

where:

L_{fv} = total equivalent length of pipe of a given size corresponding to fittings and valves of that size, ft

L_e = an equivalent length of pipe corresponding to a particular fitting or valve, ft

Values of L_e for fittings and valves are given in various references (14). Substituting Equation 3-7 for L in Equation 3-6 will result in an expression for the pressure loss due to flow through fittings and valves, or

$$\Delta P_{fv} = 645.8\ L_{fv}\left[\frac{Q}{C\ d^{2.63}}\right]^{1.85} \quad \text{(s.g.)}. \qquad (3\text{-}8)$$

Summary

The term $\rho g_o h_L/g_c$ in Equation 3-4 is now replaced by the sum of Equations 3-6 and 3-8, which when substituted back into Equation 3-4 yields the following expression for pipe flow:

$$P_1 = P_2 + \rho\frac{g_o}{g_c}(Z_2 - Z_1) + 645.8(L + L_{fv})\left[\frac{Q}{C\ d^{2.63}}\right]^{1.85} \quad \text{(s.g.)} \qquad (3\text{-}9)$$

Equation 3-9 will be used to calculate the pressures in piping segments 1-2, 2-3, 3-4, 5-6, 6-7, and 7-8 of Figure 5. The units of pressure in Equation 3-9 are lb_f/ft^2 which must be converted to units of lb_f/in^2 before use in Equation 3-1.

Cavern Flow

To develop and apply mathematical theory concerning flow within the cavern, the cavern will be subdivided into a finite number of horizontal disc shape cells as illustrated in Figure 7. Flow passes from cell to cell through the horizontal planes between adjacent cells. The outside surfaces of the cells represent the salt walls of the cavern. The analysis will result in a technique whereby the pressure drop due to flow between the cavern inlet and outlet any time during construction can be determined.

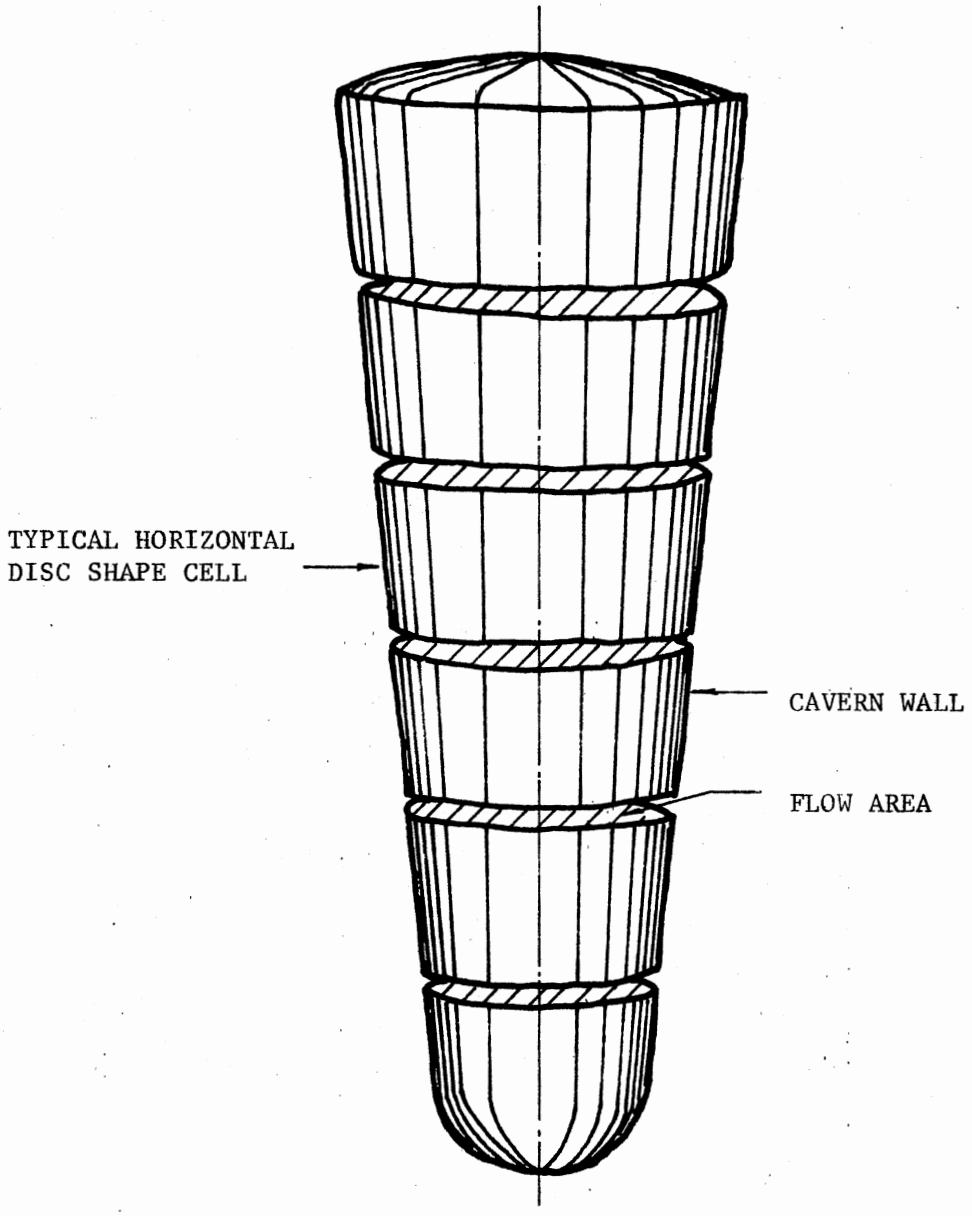

Figure 7. Typical Cavern Showing Separation Into Disc Shape Cells

Figure 8 illustrates a typical cavern cell. Equation 3-3 also applies to flow in the cell between Sections 1 and 2. Since flow in the cavern is assumed to be frictionless with the cavern wall, the term $g_o h_L$ in Equation 3-3 is set equal to zero resulting in the following expression for the pressure at Section 1.

$$P_1 = P_2 + \frac{\hat{\rho}(V_2^2 - V_1^2)}{2g_c} + \frac{\hat{\rho} g_o}{g_c}(Z_2 - Z_1) \qquad (3\text{-}10)$$

where $\hat{\rho}$ is the average mass density of the fluid in the cavern cell and is calculated by multiplying the mass density of water by the average specific gravity of the fluid in the cell.

The average specific gravity for the fluid in each cell is calculated in Saberian's simulation program. The cell section elevations Z_1 and Z_2 are defined system geometry. The calculation procedure is designed to determine the pressure at Section 2 of a cell prior to calculation of P_1; therefore P_2 is always known. The calculation of fluid velocities V_1 and V_2 will now be discussed as an integral part of and resulting from the process of dissolving salt.

The Dissolution Process

The objectives of the following discussion are to 1) explain how a cell is enlarged over time, and 2) show how to determine the velocities at Sections 1 and 2. The discussion of the dissolution process will be based on the volume unit of a gallon, although other units could as easily be used.

The volume of fluid leaving a cell during leaching will always be less than the volume of fluid entering the cell assuming a constant temperature process. The only exception to this is when the fluid is

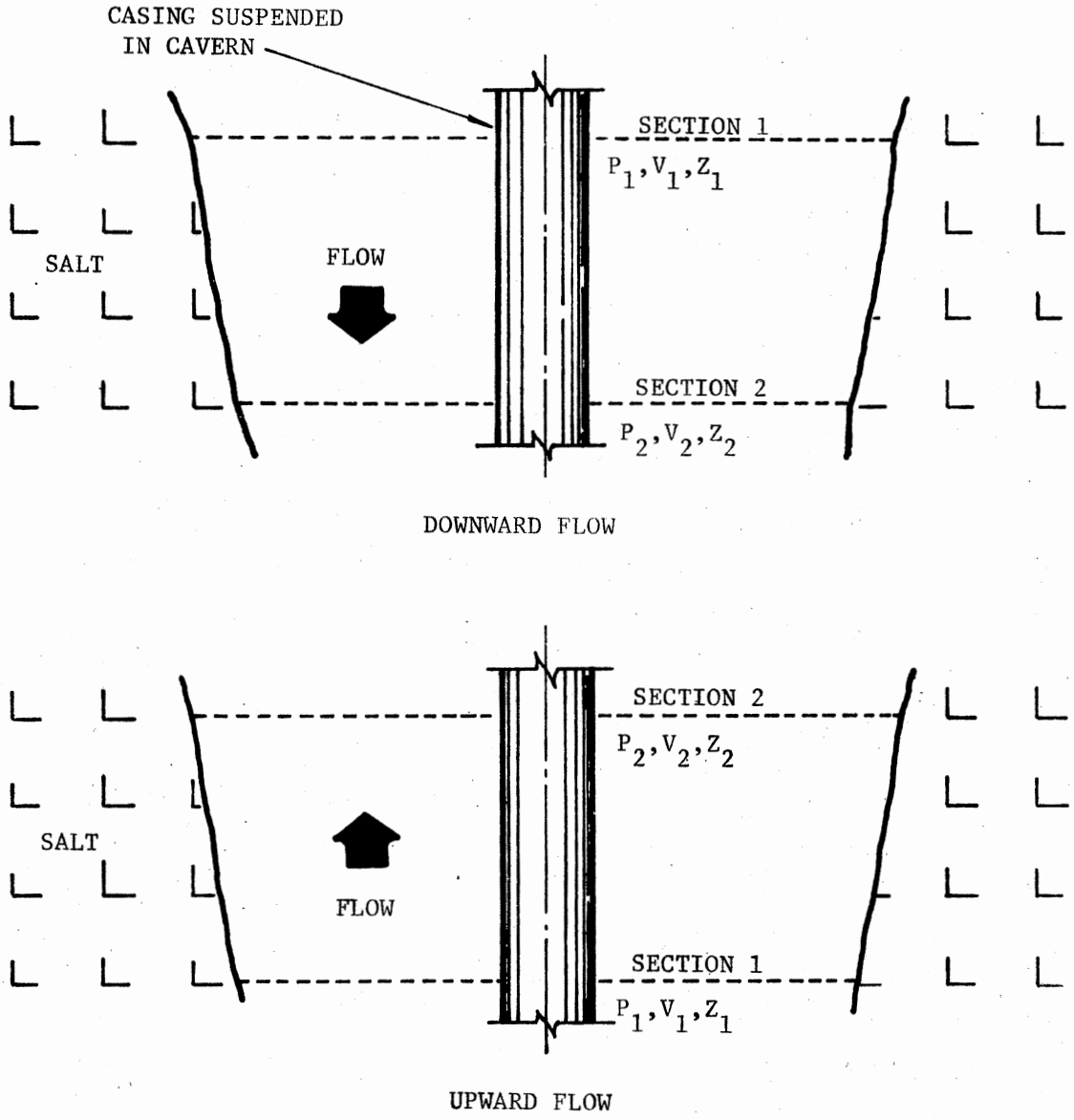

Figure 8. Typical Cavern Cells for Upward and Downward Flow

100 percent saturated in which case no dissolution occurs, therefore the volume of fluid entering the cell is equal to the fluid volume leaving the cell. For each gallon of fluid (fresh water or partially saturated brine) entering a cavern cell, an amount of salt will be dissolved from the cavity wall, thus increasing the cell volume.

Also, the fluid that is produced by mixing of the dissolved salt with the original gallon of fluid entering the cell has a volume in excess of one gallon. For solution mining of salt dome cavities the chemical dissolution process is such that the increase in volume of new space created (volume of salt dissolved) is always greater than the increase in volume of the leaving fluid. For this reason the volume of fluid leaving a cell is always less than the volume of fluid entering the cell.

A ratio may be defined relating the volume of fluid leaving a cell to the volume of fluid entering the same cell. A sample calculation is given in Appendix A to illustrate the procedure and logic used to calculate such a ratio for any cell when the specific gravity of brine both entering and leaving the cell is known.

In order to avoid storing in computer memory the tables of brine properties (Table IX) necessary to calculate a given volumetric ratio, an equation was developed by this researcher to directly calculate the ratio. Three different brine properties are estimated using predicting polynomials based on a Taylor series expansion and a least squares criterion.

The resulting expression is:

$$\text{RATIO} = \frac{K3}{K4} - 0.0554813[(K3)(K6) - K5] \qquad (3\text{-}11)$$

where:

K1 = specific gravity of brine entering the cell

K2 = specific gravity of brine leaving the cell

and

$$K3 = 0.798243 + 0.847665\ (K1) - 0.645048\ (K1)^2$$

$$K4 = 0.798243 + 0.847665\ (K2) - 0.645048\ (K2)^2$$

$$K5 = -6.658631 + 1.266359\ (K1) + 5.385055\ (K1)^2$$

$$K6 = 3.855827 - 19.339687\ (K2) + 15.482495\ (K2)^2$$

Equation 3-11 is a volumetric ratio and is used to relate flow at Section 1 and 2 of a given cell as follows:

$$\text{flow rate at Section 2} = \text{RATIO}\left[\text{flow rate at Section 1}\right], \text{ or}$$

$$A_2V_2 = \text{RATIO}(A_1V_1). \tag{3-12}$$

Solving Equation 3-12 for V_1 yields the following expression for which the values for all variables on the right hand side can be determined prior to calculation of V_1:

$$V_1 = \frac{1}{\text{RATIO}} \frac{A_2}{A_1} V_2. \tag{3-13}$$

Saberian's simulation program generates values for the specific gravity and radius at the midpoint of each cell as shown in Figure 9. In order to calculate values for the ratio and the areas in Equation 3-13 the specific gravity and radius must be known at Sections 1 and 2 of each cell. This is accomplished by using average values determined with the following set of equations illustrated for a typical Cell B in Figure 9:

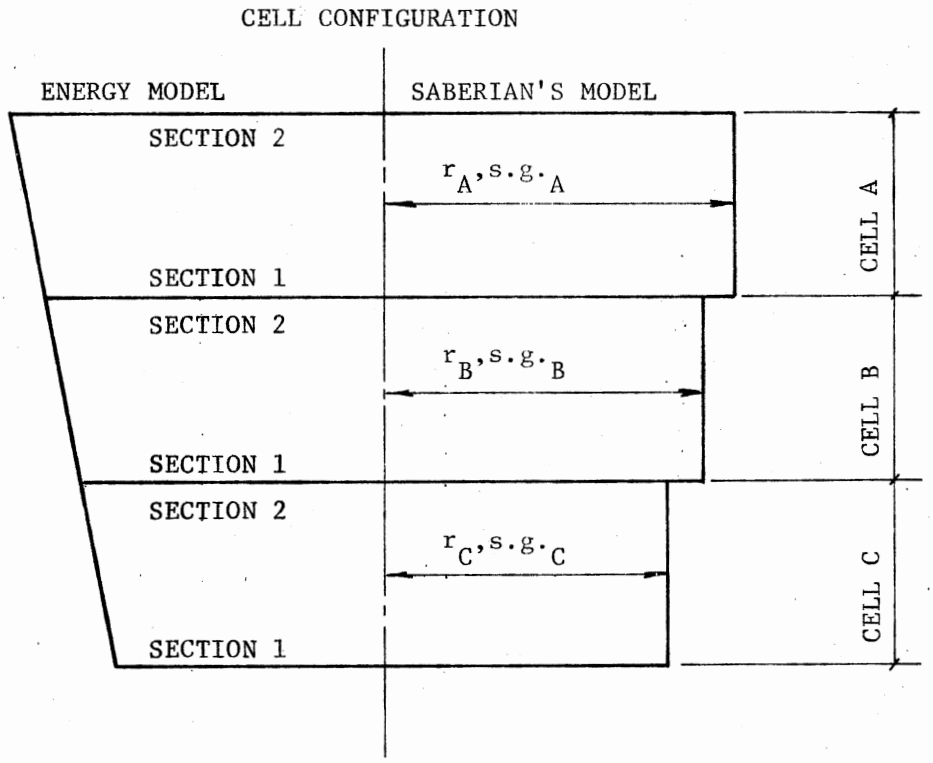

Figure 9. Comparison of Cell Configuration Between Saberian's Model and Energy Model

$$\text{Radius at Section 1} = r_1 = \frac{r_B + r_C}{2} \qquad (3\text{-}14)$$

$$\text{Radius at Section 2} = r_2 = \frac{r_A + r_B}{2} \qquad (3\text{-}15)$$

$$\text{Specific gravity at Section 1} = s.g._1 = \frac{s.g._B + s.g._C}{2} \qquad (3\text{-}16)$$

$$\text{Specific gravity at Section 2} = s.g._2 = \frac{s.g._A + s.g._B}{2} \qquad (3\text{-}17)$$

This model defines the radius and specific gravity at the bottom section of the bottom cell to be equal to the corresponding values at the midpoint of the same cell. Likewise, the radius and specific gravity at the top section of the top cell are defined to be equal to corresponding values at the midpoint of the top cell.

Given radii at Sections 1 and 2 for a cell, then the circular areas A_1 and A_2 required in Equation 3-13 are easily calculated.

In summary, Equation 3-10 for cavern flow is the companion to Equation 3-9 for pipe flow. Both equations were developed such that an upstream pressure either in a cavern cell or a piping element can be determined given adeuqate information on downstream conditions, system geometry and the dissolution process.

CHAPTER IV

MATH MODEL

This chapter deals with developing a math model of a typical cavern construction system. Theory developed in the previous chapter will be applied to direct and reverse circulation construction techniques.

Math Model

Equations 3-9 and 3-10 will be applied to piping segments and the cavern interval respectively. The exact form of the two equations will be used although known relationships will be substituted in some cases to reduce the equations to primary factors. For example, in Equations 3-9 and 3-10 the fluid mass density ρ will be replaced by the appropriate specific gravity multiplied times the mass density of water. When the pump pressure has been determined, Equations 3-1 and 3-2 will be used to calculate energy consumption.

The pump pressure P in Equation 3-1 is also the pressure at Point 1 in Figure 5. P is determined by beginning at Point 8 and calculating pressures at various points in the system in a backwards manner until Point 1 is reached.

Nomenclature for the math model is given prior to Chapter I.

Pressure at Point 8

Point 8 is located at the entrance to the brine holding tank. The pressure at this point is the static head due to the column of fluid above the inlet. This model assumes that both the fresh water holding tank and the brine holding tank are open to the atmosphere so pressure throughout the system will be guage pressure and denoted lb_f/in^2 unless otherwise mentioned. Therefore,

$$P_8 = 0.433(sg_5)h_8 \tag{4-1}$$

The specific gravity of the fluid in the tank and in the lines leading from the tank to Point 5 in the cavern is taken as the value of the specific gravity at Point 5 at the time a calculation is made.

Pressure at Points 7, 6 and 5

When known relationships are substituted into Equation 3-9 expressions for the pressures at Points 7, 6 and 5 for pipe flow in Figure 5 become:

$$P_7 = P_8 + \left\{62.4(Z_8 - Z_7) + 645.8(L_7 + L_{fv7})\left[\frac{Q_5}{C\, d_7^{2.63}}\right]^{1.85}\right\}\frac{sg_5}{144}, \tag{4-2}$$

$$P_6 = P_7 + \left\{62.4(Z_7 - Z_6) + 645.8(L_6 + L_{fv6})\left[\frac{Q_5}{C\, d_6^{2.63}}\right]^{1.85}\right\}\frac{sg_5}{144} \tag{4-3}$$

and

$$P_5 = P_6 + \left\{62.4(Z_6 - Z_5) + 645.8(L_5 + L_{fv5})\left[\frac{Q_5}{C\, d_5^{2.63}}\right]^{1.85}\right\}\frac{sg_5}{144}. \tag{4-4}$$

where values for C and L_{fv} are determined by the user.

Pressure at Point 4

Direct Circulation. Equation 3-10 will now be applied to cavern construction using the direct circulation technique. Figure 10 shows a cavern cell classification for direct circulation, and Figure 11 shows more detail for each class of cell.

Top Cell to Casing Annulus--This model assumes that brine flows upward to Section 2 of the top cell with a uniform velocity distribution, then flows radially inward and exits from the cavern with a uniform velocity through the casing annulus at Point 5.

Applying Equation 3-10 to the flow between Section 2 of the top cell and the casing annulus results in the following expression for the pressure at Section 2:

$$P_{2,j} = P_5 + 0.013468(\hat{sg}_j)\left[\frac{V_5^2 - V_{2,j}^2}{2}\right], \quad j = n \tag{4-5}$$

where:

$$V_5 = \frac{1}{2.448}\left[\frac{Q_5}{D_I^2 - d_o^2}\right] \tag{4-6}$$

$$V_{2,j} = \frac{1}{1410.135}\left[\frac{Q_5}{R_{2,j}^2 - d_o^2/576}\right], \quad j = n \tag{4-7}$$

The specific gravity at Section 2 for this model is taken to be equal to the average specific gravity in the cell as in Saberian's model.

Top Cell, Type I--The fluid in this cell is assumed to pass through Section 1 with uniform velocity across area A_1, perform its dissolution work in the cell, then flow to Section 2 with a uniform velocity

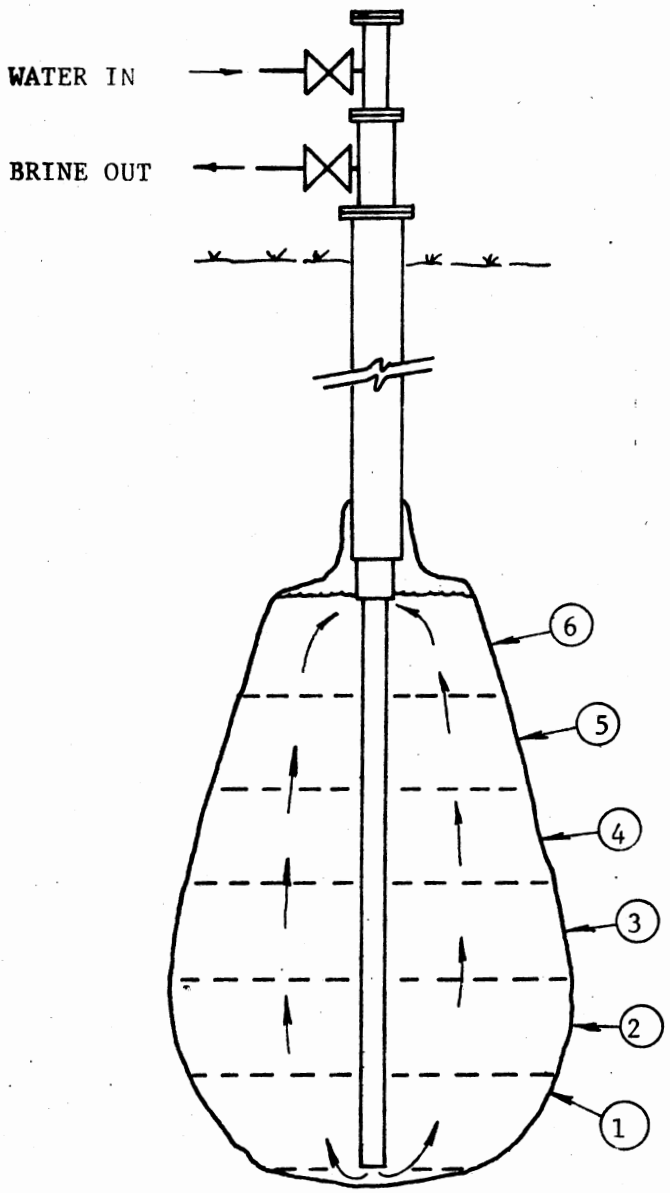

CELL NO.	CLASSIFICATION
1	BOTTOM CELL, TYPE I
2 - 5	INTERMEDIATE CELL, TYPE I
6	TOP CELL, TYPE I

Figure 10. Cell Classification for Direct Circulation

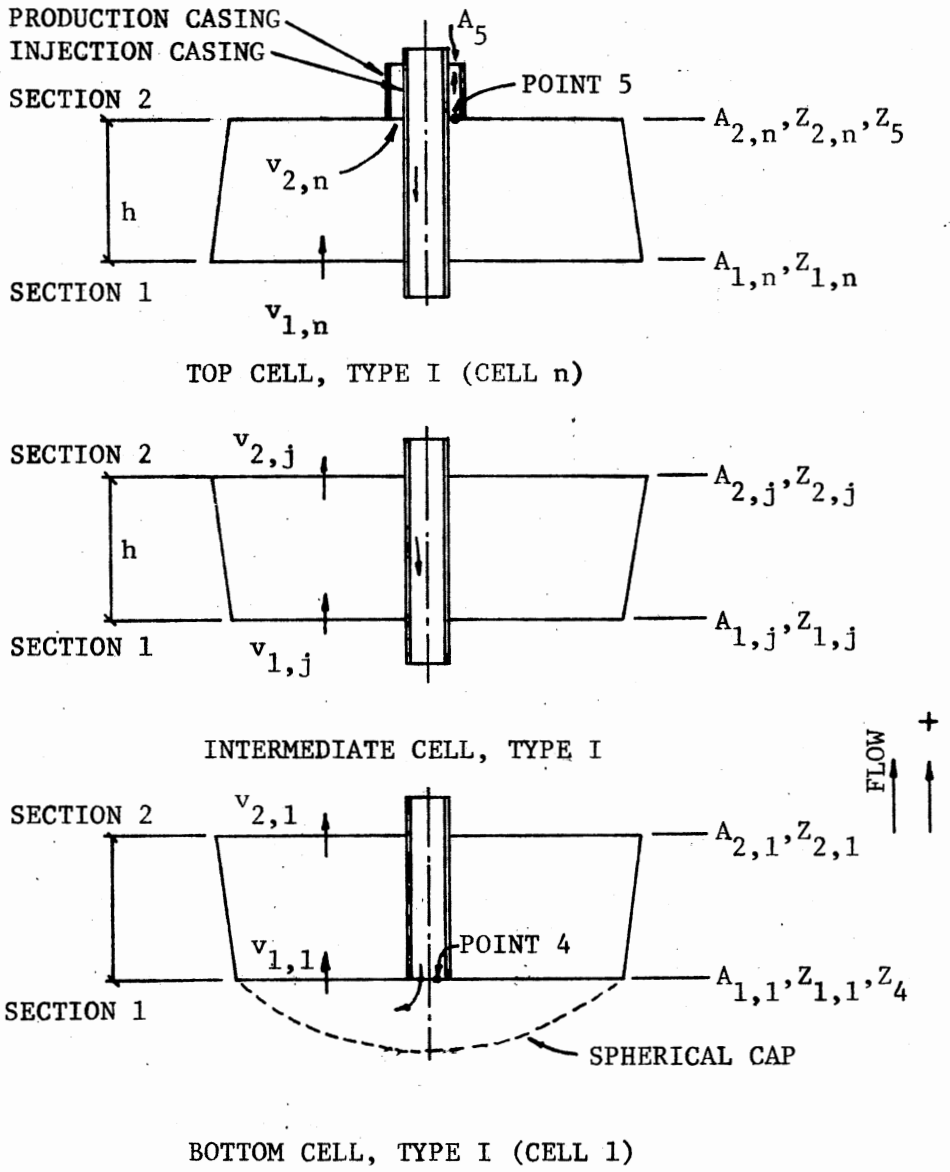

Figure 11. Detail of Cavern Cells for Direct Circulation

distribution. The top cell is always denoted Cell n, where n is the total number of cells.

Applying Equation 3-10 to the top cell yields the following expression for the pressure at Section 1.

$$P_{1,j} = P_{2,j} + 0.013468(\hat{sg}_j)\left\{\frac{V_{2,j}^2 - V_{1,j}^2}{2} + 32.174(Z_5 - Z_{1,j})\right\}, \quad j = n \tag{4-8}$$

where:

$$V_{1,j} = \frac{1}{1410.135}\left[\frac{Q_5/R_j}{R_{1,j}^2 - d_o^2/576}\right], \quad j = n \tag{4-9}$$

and $V_{2,n}$ is given by Equation 4-7.

Intermediate Cell Type I--Flow is assumed to enter an intermediate cell with uniform velocity across Section 1 and leave with uniform velocity across Section 2. Figure 11 shows such a cell with area A_2 greater than area A_1. The reverse could also be true as shown in Figure 10. Saberian's simulation program generates the cell radii at incremental time steps.

Equation 3-10 is applied directly to an intermediate cell to yield the following expression for the pressure at Section 1.

$$P_{1,j} = P_{2,j} + 0.013468(\hat{sg}_j)\left\{\frac{V_{2,j}^2 - V_{1,j}^2}{2} + 32.174(Z_{2,j} - Z_{1,j})\right\} \tag{4-10}$$

where:

$$V_{1,j} = \frac{1}{1410.135}\left[\frac{Q_{2,j}/R_j}{R_{1,j}^2 - d_o^2/576}\right] \tag{4-11}$$

$$V_{2,j} = \frac{1}{1410.135}\left[\frac{Q_{2,j}}{R_{2,j}^2 - d_o^2/576}\right] \qquad (4\text{-}12)$$

Bottom Cell, Type I--For direct circulation the bottom cell will always be denoted as Cell 1. This model assumes that water flowing from the injection casing reverses its direction of flow in the sperical cap and flows past Section 1 of the bottom cell with a uniform velocity distribution. The fluid performs its dissolution process and leaves the cell uniformly through Section 2. Equations 4-10 through 4-12 are used to calculate the pressure at Section 1 of the bottom cell, by defining the subscript j to equal 1.

Spherical Cap--Applying Equation 3-10 to flow in the spherical cap results in the following expression for the pressure at the bottom of the injection casing:

$$P_4 = P_{1,j} + 0.013468\left[\frac{\hat{sg}_j + sg_4}{2}\right]\left[\frac{V_{1,j}^2 - V_4^2}{2}\right], \quad j = 1 \qquad (4\text{-}13)$$

where:

$$V_{1,j} = \frac{1}{1410.135}\left[\frac{Q_{2,j}/R_j}{R_{1,j}^2 - d_o^2/576}\right], \quad j = 1 \qquad (4\text{-}14)$$

$$V_4 = \frac{1}{2.448}\left[\frac{Q_{2,j}/(R_j \times R_{cap})}{d_I^2}\right], \quad j = 1 \qquad (4\text{-}15)$$

Saberian's model does not define a fluid specific gravity at Section 1 of the same cell. Therefore, the average specific gravity in the bottom cell is defined in this model to be the specific gravity at Section 1 of the same cell.

Reverse Circulation, Top Cavern Injection. Figure 12 shows a cell classification for cavern construction using reverse circulation with the fresh water injected at the top of the cavern. Figure 13 illustrates more detail for each class of cell.

The general flow scheme for this construction technique is reversed to that used in direct circulation. Salt wall dissolution occurs in all cells except when the brine is saturated.

Spherical Cap--The change in direction from downward flow at Section 2 of the bottom cell to upward flow at Point 5 in the production casing occurs in the spherical cap. Equations 4-5 and 4-7 are used to determine the pressure and velocity at Section 2 of the bottom cell by defining the subscript j equal to 1. The velocity at Point 5 is defined by

$$V_5 = \frac{1}{2.448}\left[\frac{Q_5}{d_I^2}\right]. \qquad (4\text{-}16)$$

Bottom Cell, Type II--As fluid moves through this cell, uniform velocity distributions are assumed over areas A_1 and A_2. Equation 4-8 is used to determine the pressure at Section 1 of the bottom cell, while Equations 4-7 and 4-9 define velocities $V_{2,j}$ and $V_{1,j}$ respectively. The subscript j in the above equations is set equal to 1 for this cell.

Intermediate Cell, Type II--Flow through a Type II intermediate cell is the same as through a Type I intermediate cell except the direction is reversed. Equation 4-10 through 4-12 apply to flow in an intermediate cell.

Top Cell, Type II--This model assumes that fluid is injected into the cavern from the casing annulus and enters the top cell through Section 1 with a uniform velocity distribution. Equations 4-10 through

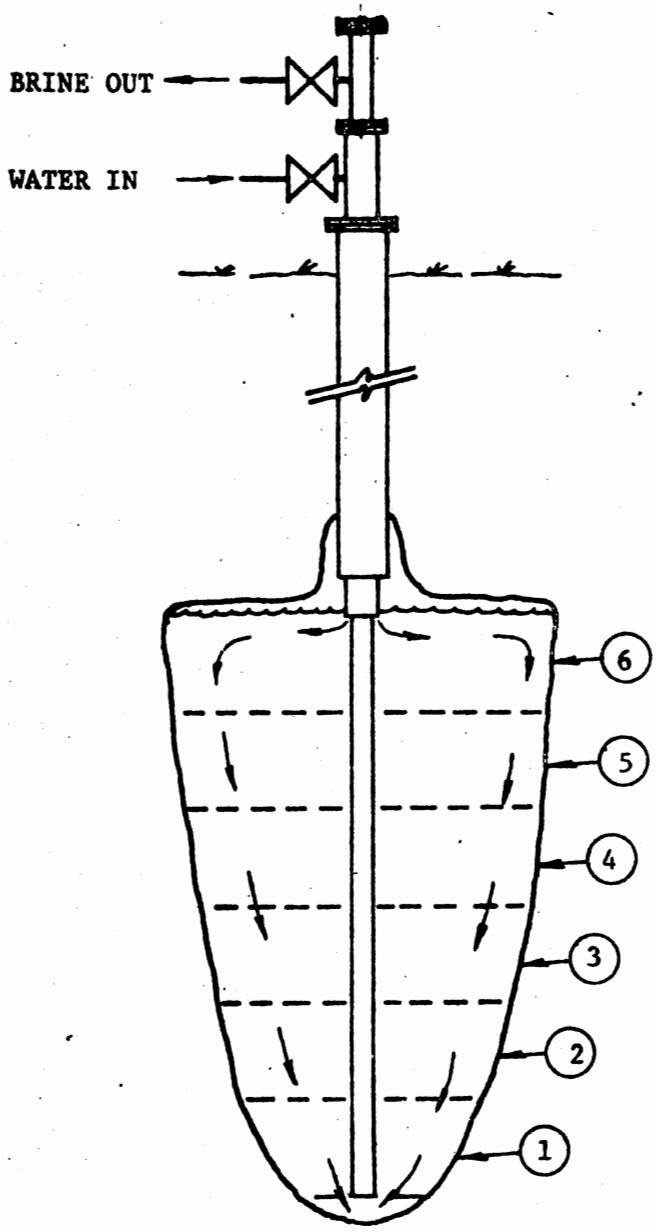

CELL NO.	CLASSIFICATION
1	BOTTOM CELL, TYPE II
2 - 5	INTERMEDIATE CELL, TYPE II
6	TOP CELL, TYPE II

Figure 12. Cell Classification for Reverse Circulation

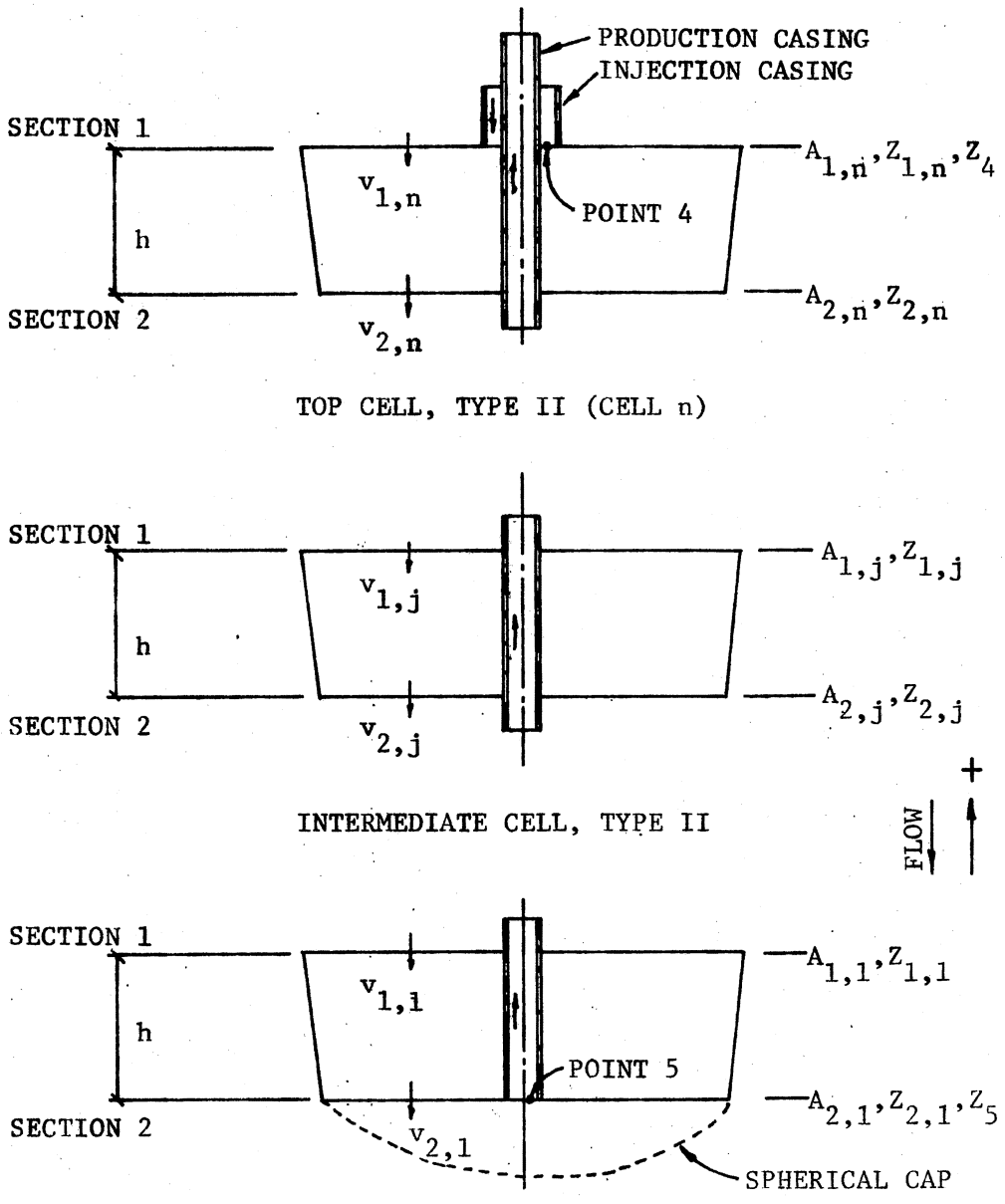

Figure 13. Detail of Cavern Cells for Reverse Circulation

4-12 are used to calculate the pressure at Section 1 of this cell by setting the subscript j equal to n.

Casing Annulus to Top Cell--For this construction technique fluid is injected into the cavern at Point 4 through the casing annulus then is assumed to be distributed uniformly over $A_{1,n}$. The pressure at Point 4 and the velocity at Section 1 of the top cell are calculated using Equations 4-13 and 4-14 by defining the subscript j equal to n. The velocity in the annulus is calculated using the following equation.

$$V_4 = \frac{1}{2.448}\left[\frac{Q_{2,n}/R_n}{D_I^2 - d_o^2}\right], \quad j = n \qquad (4\text{-}17)$$

Reverse Circulation, Mid-Cavern Injection. Mid-cavern injection refers to a reverse circulation technique with the injection casing set at any level within the cavern except at the top or bottom of the cavern interval. Figure 14 shows a cell classification for cavern construction using this technique with fluid being injected at the interface of an upper intermediate cell and a lower intermediate cell. Figure 15 illustrates more detail for each class of cell. The only difference in an upper and lower intermediate cell is the largest diameter casing suspended through the cell.

Spherical Cap--Equations 4-5, 4-7 and 4-16 are used to solve for the pressure at Section 2 of the bottom cell by setting j = 1.

Bottom Cell, Type II--Equations 4-7, 4-8 and 4-9 are applied to the bottom cell by letting j = 1.

Lower Intermediate Cell, Type II--Equations 4-10, 4-11 and 4-12 are applied to a cell of this type.

Upper Intermediate Cell, Type II--Equation 4-10 is also applied to upper intermediate cells. The corresponding equations defining the

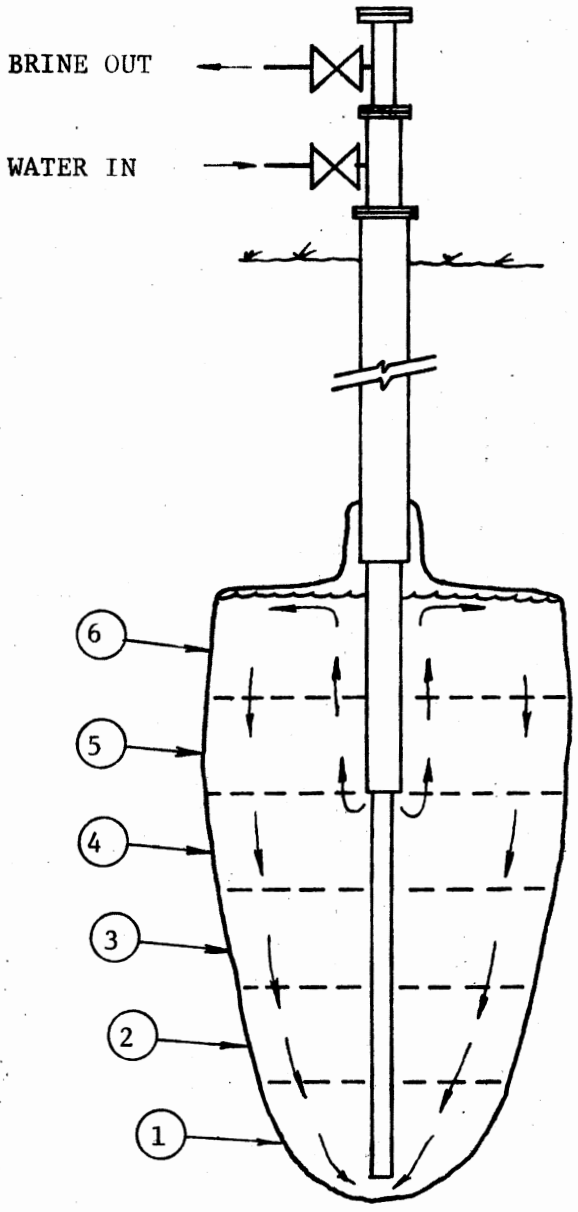

CELL NO.	CLASSIFICATION
1	BOTTOM CELL, TYPE II
2,3,4	LOWER INTERMEDIATE CELL, TYPE II
5	UPPER INTERMEDIATE CELL, TYPE II
6	TOP CELL, TYPE II

Figure 14. Cell Classification for Reverse Circulation, Mid-Cavern Injection

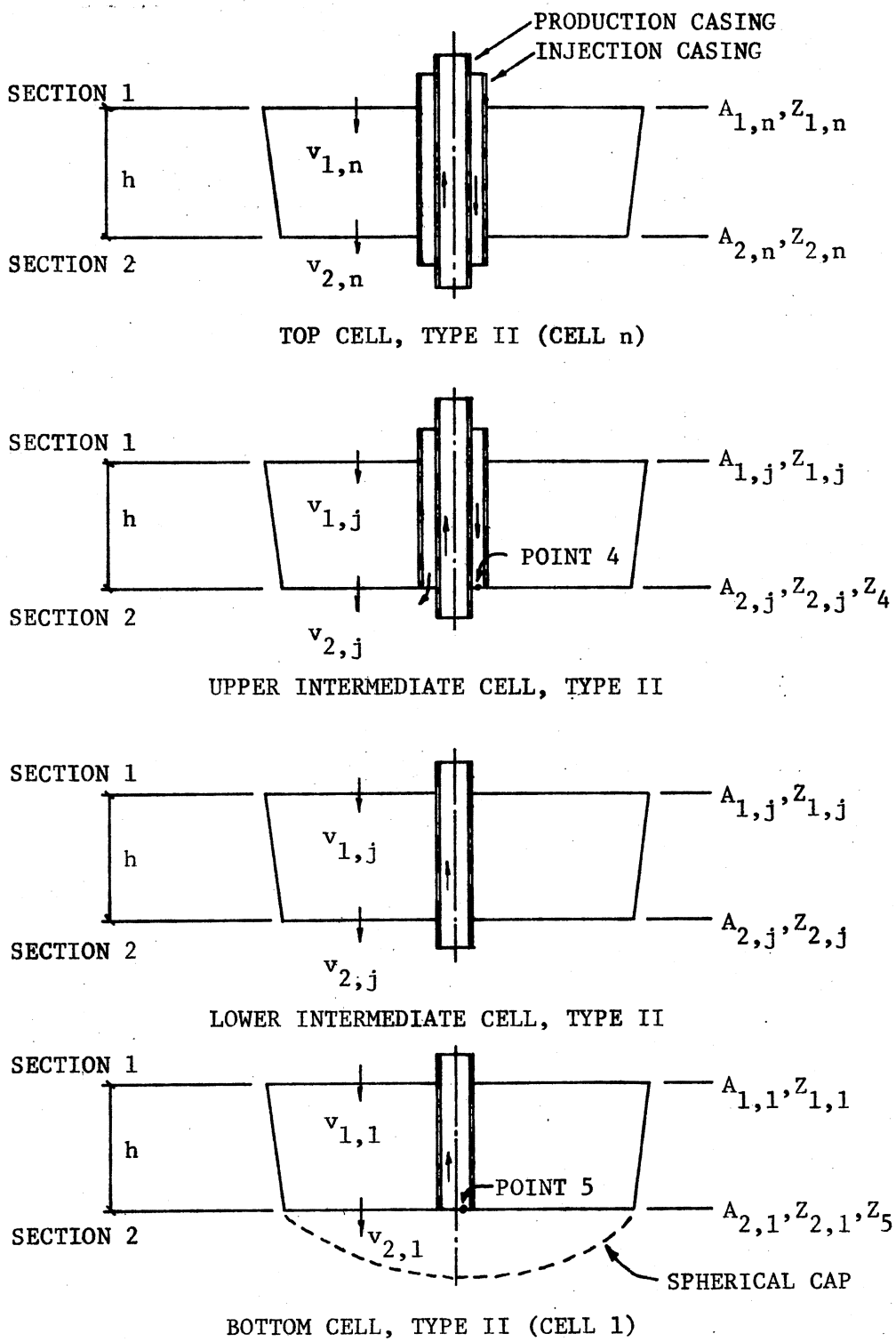

Figure 15. Detail of Cavern Cells for Reverse Circulation, Mid-Cavern Injection

velocities at Sections 1 and 2 differ from Equations 4-11 and 4-12 only in the diameter of the casing suspended in the cavern cell. Therefore, the velocity equations are given as

$$V_{1,j} = \frac{1}{1410.135}\left[\frac{Q_{2,j}/R_j}{R_{1,j}^2 - D_o^2/576}\right], \text{ and} \tag{4-18}$$

$$V_{2,j} = \frac{1}{1410.135}\left[\frac{Q_{2,j}}{R_{2,j}^2 - D_o^2/576}\right]. \tag{4-19}$$

Top Cell, Type II--As for the case of the top cavern injection, the top cell for mid cavern injection is denoted Cell n. This model assumes that fluid enters the cell with a uniform distribution over area $A_{1,n}$, performs its work of dissolution, then leaves the cell through $A_{2,n}$. Equations 4-10, 4-18 and 4-19 are used to calculate the pressure at Section 1 of the top cell by defining the subscript j equal to n.

Casing Annulus to Top Cell--For this construction technique fluid is injected at Point 4 located at some elevation in the cavern interval between the cavern floor and roof. It travels upward to the cavern roof where this model assumes that it then spreads radially outward and enters the top cell through area $A_{1,n}$ with a uniform velocity distribution.

Equation 3-10 applied to this situation yields the following expression for the pressure at Point 4:

$$P_4 = P_{1,n} + 0.013468\left[\frac{\hat{sg}_n + sg_4}{2}\right]\left\{\frac{V_{1,n}^2 - V_4^2}{2} + 32.174(Z_{1,n} - Z_4)\right\}, \tag{4-20}$$

where $V_{1,n}$ is given by Equation 4-18 and V_4 is given by Equation 4-17 by defining j equal to n.

Pressure at Point 3, 2 and 1

When known relationships are substituted into Equation 3-9, the expressions for the pressures at Points 3, 2 and 1 for pipe flow in Figure 5 become:

$$P_3 = P_4 + \left\{62.4(Z_4 - Z_3) + 645.8(L_3 + L_{fv3})\left[\frac{Q_4}{C\ d_3^{2.63}}\right]^{1.85}\right\}\frac{sg_1}{144}, \tag{4-21}$$

$$P_2 = P_3 + \left\{62.4(Z_3 - Z_2) + 645.8(L_2 + L_{fv2})\left[\frac{Q_4}{C\ d_2^{2.63}}\right]^{1.85}\right\}\frac{sg_1}{144} \tag{4-22}$$

and

$$P_1 = P_2 + \left\{62.4(Z_2 - Z_1) + 645.8(L_1 + L_{fv1})\left[\frac{Q_4}{C\ d_1^{2.63}}\right]^{1.85}\right\}\frac{sg_1}{144}. \tag{4-23}$$

Hydraulic Power Requirement

When the pressure at Point 1 has been determined, Equation 3-1 is used to calculate the hydraulic power in kilowatts required to maintain flow rate Q, and is expressed as

$$P_r = \frac{(P_1)(Q_4)}{2298.5} \tag{4-24}$$

Energy Consumed

The energy consumed during time interval ΔT at power level P_r is expressed using Equation 3-2 as:

$$E_{\Delta T} = (P_r)(\Delta T). \tag{4-25}$$

Computer Program

To aid in the calculation of energy consumption during simulated cavern construction, a FORTRAN computer program was developed incorporating Saberian's simulation program. For a given set of input data including desired cavern size the program output includes the daily power level and accumulative energy consumption.

The program was developed for an IBM SYSTEM 370/158 central processing unit, and was executed using a FORTRAN G1 compiler. All cavern construction simulations were run with a memory allocation of 200K. A copy of the program listing is on file with Dr. James E. Shamblin of the Department of Industrial Engineering and Management at Oklahoma State University.

CHAPTER V

TECHNICAL INVESTIGATION

In this chapter the research objective is formulated as a mathematical problem and solved.

It is common for the client who desires cavern storage space to want it as quickly as possible. By knowing the time that it takes to construct a pumping plant and do the necessary drilling and the time that cavern construction must be completed, gives the time allowable for cavern construction. The total amount of water that must be pumped underground in order to create the desired amount of cavern space can be estimated. Dividing the volume of water to be pumped by the time allowed for pumping gives the pumping capacity (rate) for which the pumping plant must be designed.

During actual field construction when a cavern sump is being built, it is common to use total pumping capacity as soon as circulation is established and a small amount of space has initially been created. It is also common that the brine produced from sump construction is unsaturated because the fast pumping rate does not allow the water enough exposure time in the sump to dissolve all the salt that it could otherwise. During cavern construction, total pumping capacity is always used.

It is the objective of this research to remove construction time limitations and consider the problem of controlling the pumping rate through time to efficiently construct a sump and cavern of given size

while minimizing total energy consumed and minimizing construction time. Later in this cahpter the objective will be expressed mathematically for the purpose of this investigation.

Description of Test Construction System

The test construction system used in this research has constant numerical values given to each input variable except flow rate. Sample parameter values were selected for the case of constructing a medium-size cavern of up to approximately four million barrels of usable space in a medium-depth salt dome.

Sump Construction

Figure 16 illustrates the test construction system used for sump construction. Actually, not only is the sump being constructed, but the central core of the cavern as well. It is assumed that the salt contains 8-10% insoluble material, such as sand, so a volume of space from 320,000 to 400,000 barrels must be constructed in the interval between 2,500 and 2,850 feet. This sump is therefore sized to hold the insoluable material produced from cavern construction.

Sump construction begins from an initial borehole diameter of 16 inches and an assumed constant specific gravity in the borehole of 1.00.

Cavern Construction

Figure 17 illustrates the test construction system used for cavern construction. The production casing has been positioned at 2,500 feet and the injection casing is positioned at 2,300 feet. Cavern construction

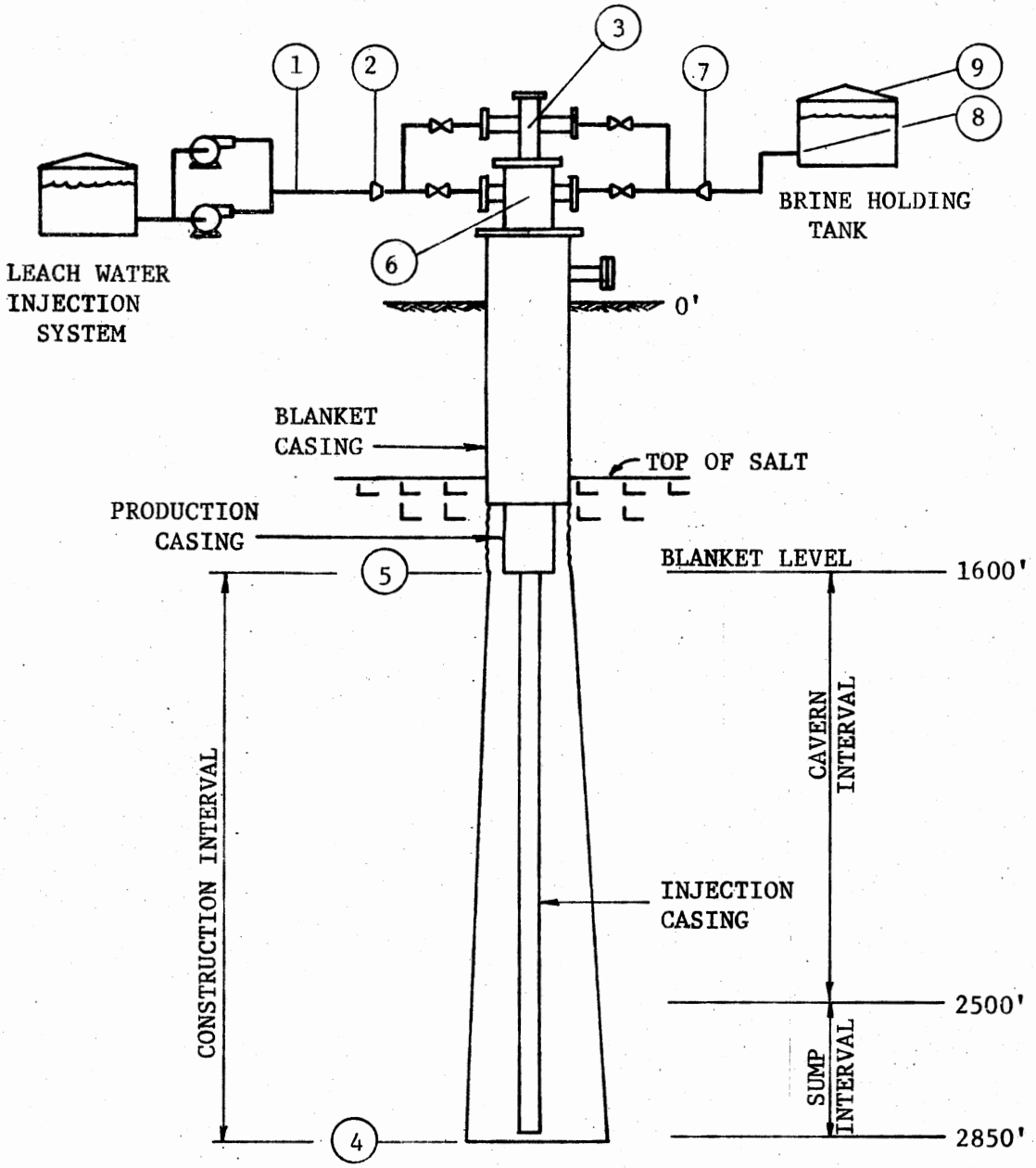

Figure 16. Sump Construction Using Direct Circulation

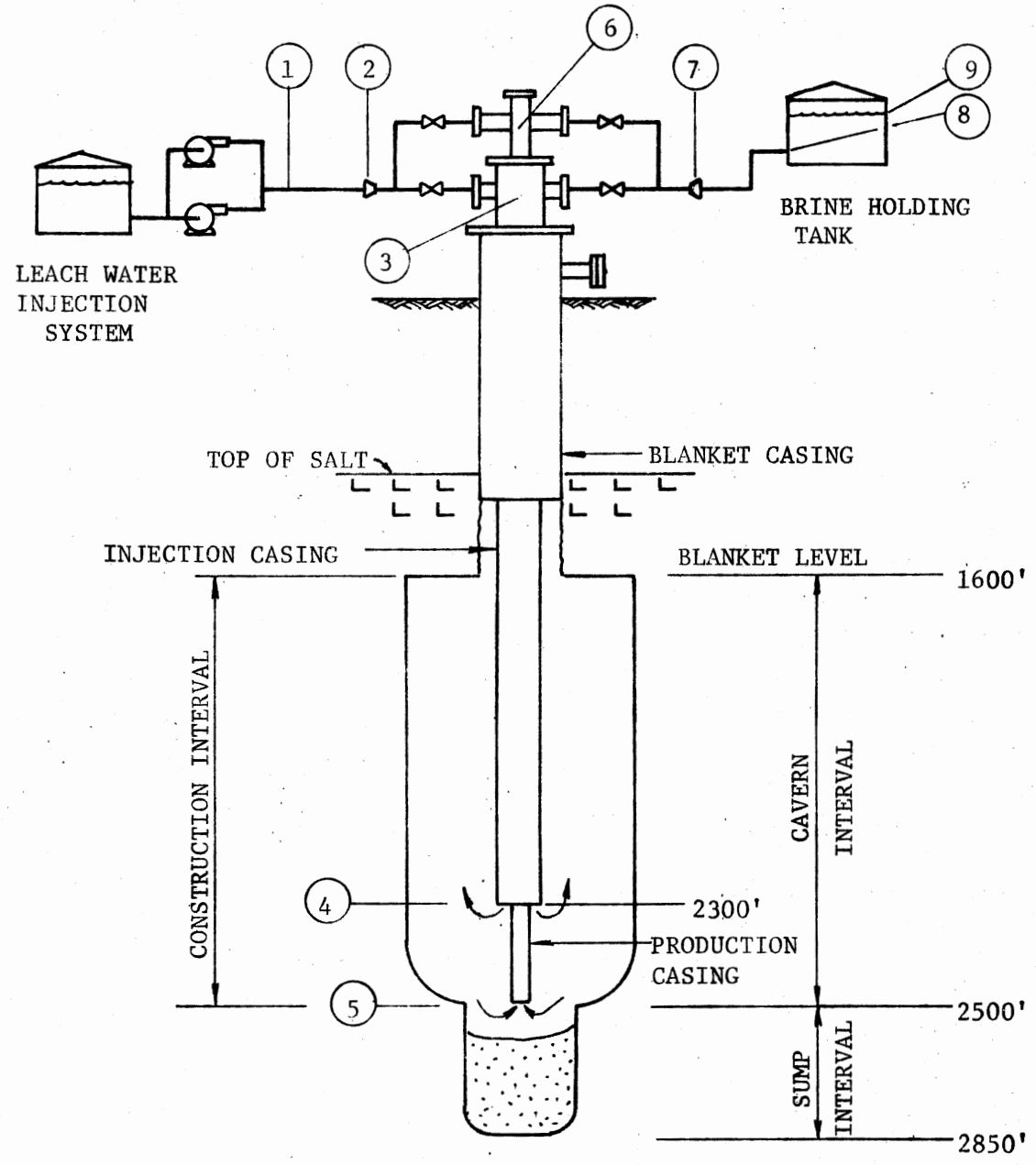

Figure 17. Cavern Construction Using Reverse Circulation, Mid-Cavern Injection

is allowed to continue until four million barrels of space is created between 1,600 and 2,500 feet.

Cavern construction begins from the central core developed during sump construction. The radius and specific gravity of the core at various elevations represent a starting condition determined after the sump construction calculations have been performed.

Tables I, II and III give the numerical values used for the input data for sump and cavern construction calculations.

TABLE I

GENERAL INPUT DATA FOR SUMP AND CAVERN CONSTRUCTION

Variable	Sump Construction	Cavern Construction
Construction interval, ft	1250	900
Depth to blanket level, ft	1600	1600
Outside diameter of large suspended casing, in	20	20
Inside diameter of large suspended casing, in	18.927	18.927
Outside diameter of small suspended casing, in	13.375	13.375
Inside diameter of small suspended casing, in	12.615	12.615
Equivalent diameter of casing annulus, in	11.170	11.170
Specific gravity of injection water	1.000	1.000
Specific gravity of brine in borehole	1.000	see text
Specific gravity of rock salt	2.165	2.165
No. of disc-shaped computational cells	25	18

TABLE II

INPUT DATA FOR SUMP CONSTRUCTION

Point (I)	D(I) Inches	XL(I) Feet	ELFV(I) Feet	E(I) Feet
1	15.250	2000	191	5
2	12.000	10	177	7
3	12.615	2862	79	12
4	--	--	--	-2850
5	11.170	1607	70	-1600
6	12.000	5	117	7
7	17.250	2000	309	7
8	--	--	--	5
9	--	--	--	25

Where:

D(I) = internal diameter of pipe between Points I and I + 1.
XL(I) = length of piping segment between Points I and I + 1.
ELFV(I) = equivalent length of fittings and valves between Points I and I + 1.
E(I) = elevation of Point I.

TABLE III

INPUT DATA FOR CAVERN CONSTRUCTION

Point (I)	D(I) Inches	XL(I) Feet	ELFV(I) Feet	E(I) Feet
1	15.250	2000	191	5
2	12.000	5	117	7
3	11.170	2307	70	7
4	--	--	--	-2300
5	12.615	2512	79	-2500
6	12.000	10	177	12
7	17.250	2000	309	7
8	--	--	--	5
9	--	--	--	25

See Table II for variable definitions.

Piping sizes were chosen for a maximum brine production rate of 3,000 gallons per minute.

Solution of Research Objectives

A "baseline" case will be defined and used as a basis of comparison for subsequent work.

Baseline Case

This case is the basis on which all other tests formulated for this study will be evaluated. As mentioned earlier, it is common to use total pumping capacity throughout the construction phase. The computer program developed for this research was used to simulate the construction

of a cavern with a usable volume of approximately 4,000,000 barrels and a sump with a volume about 400,000 varrels. The simulation was carried out with a constant brine production rate of 3,000 gpm. Table IV lists some of the data generated from the simulated activity.

TABLE IV

RESULTS FROM BASELINE SIMULATION

Sump volume	402,026 bbls
Sump construction time	88 days
Energy consumed	620,891 kw-hrs
Cavern volume	4,005,003 bbls
Cavern construction time	268 days
Energy consumed	1,929,946 kw-hrs

Figure 18 illustrates the final shape of the cavern and sump. The sump profile is shown as a dotted line indicating that it would be filled if all of the expected insolubles were accumulated.

Constant Flow Rate Cases

The impact on total energy consumption as a function of different constant flow rates was investigated. Nine construction simulations were run using produced brine flow rates from 300 to 2,700 gpm in 300 gpm increments. Table V gives some results of the simulation runs with the last row representing the baseline case from Table IV.

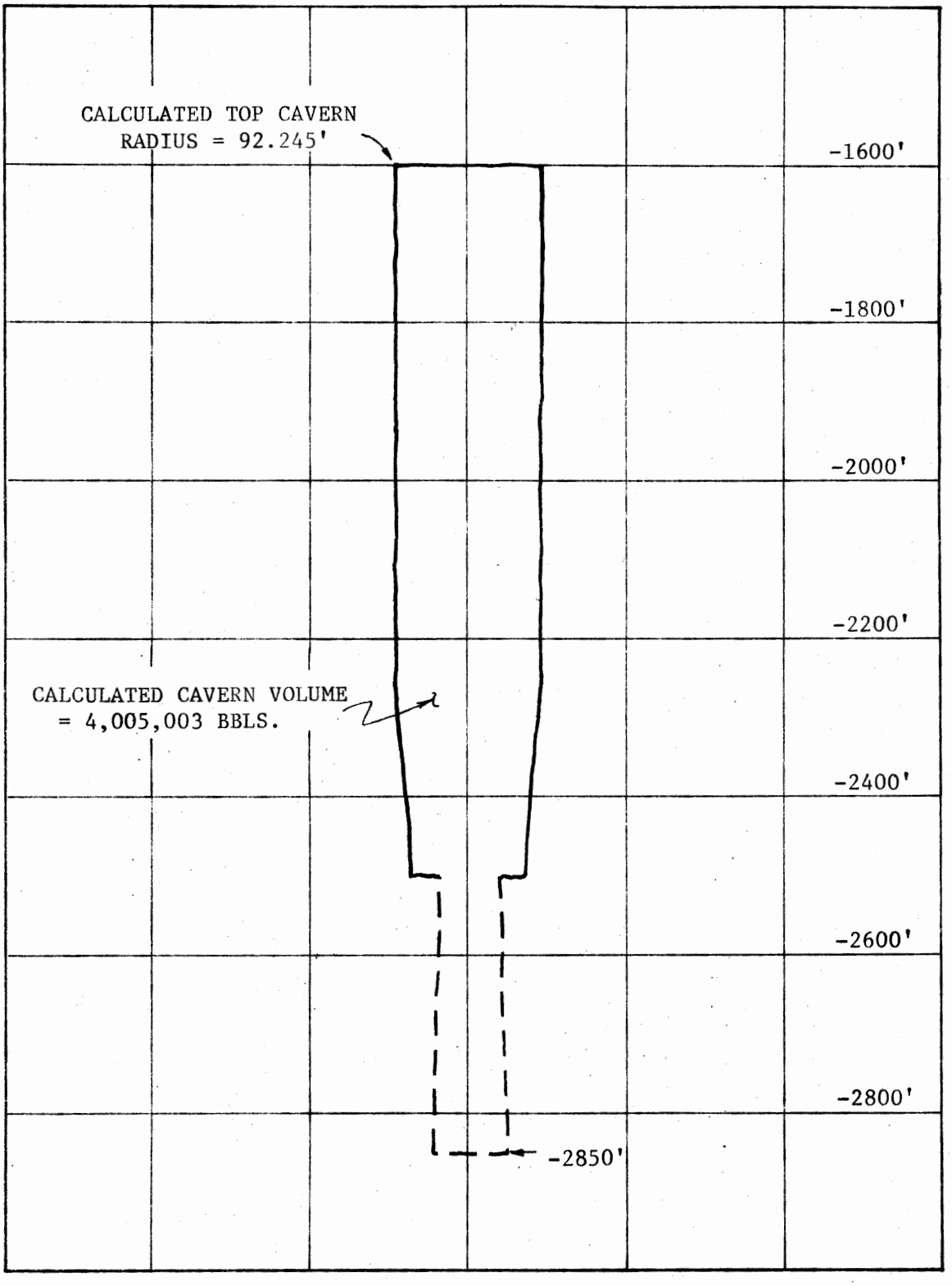

Figure 18. Final Shape of Cavern and Sump for Baseline Case

TABLE V

RESULTS FROM SIMULATIONS USING CONSTANT FLOW RATE POLICIES

Flow Rate, gpm	Sump			Cavern		
	Volume, bbls	Construction Time, days	Energy Consumed, kw-hrs	Volume, bbls	Construction Time, days	Energy Consumed, kw-hrs
300	400,945	331	258,330	4,000,112	2,241	1,326,543
600	400,184	191	281,071	4,001,263	1,158	1,357,840
900	400,656	146	308,515	4,004,869	793	1,394,027
1,200	400,820	125	341,796	4,001,672	607	1,435,339
1,500	401,916	112	375,748	3,999,997	495	1,488,355
1,800	403,308	104	415,881	4,001,290	420	1,553,489
2,100	402,081	98	458,016	4,000,870	366	1,629,600
2,400	403,466	94	507,898	4,010,168	326	1,721,431
2,700	404,373	91	563,970	4,011,520	294	1,821,058
3,000	402,026	88	620,891	4,005,003	268	1,929,946

The final shape of the cavern and sump for each of the nine simulation runs were very similar to the final shape generated for the baseline case. All the cavern shapes approached a cylinder, and the top cavern radii varied between 88 and 95 feet.

Information generated from the baseline case and the constant flow rate cases was used to construct curves and provide coefficients for equations used throughout this chapter.

Constraints on Flow Rate. Figure 19 shows a plot for the sump construction time and energy savings as a function of the produced brine flow rate. At a flow rate of 300 gpm, the construction time of 331 days

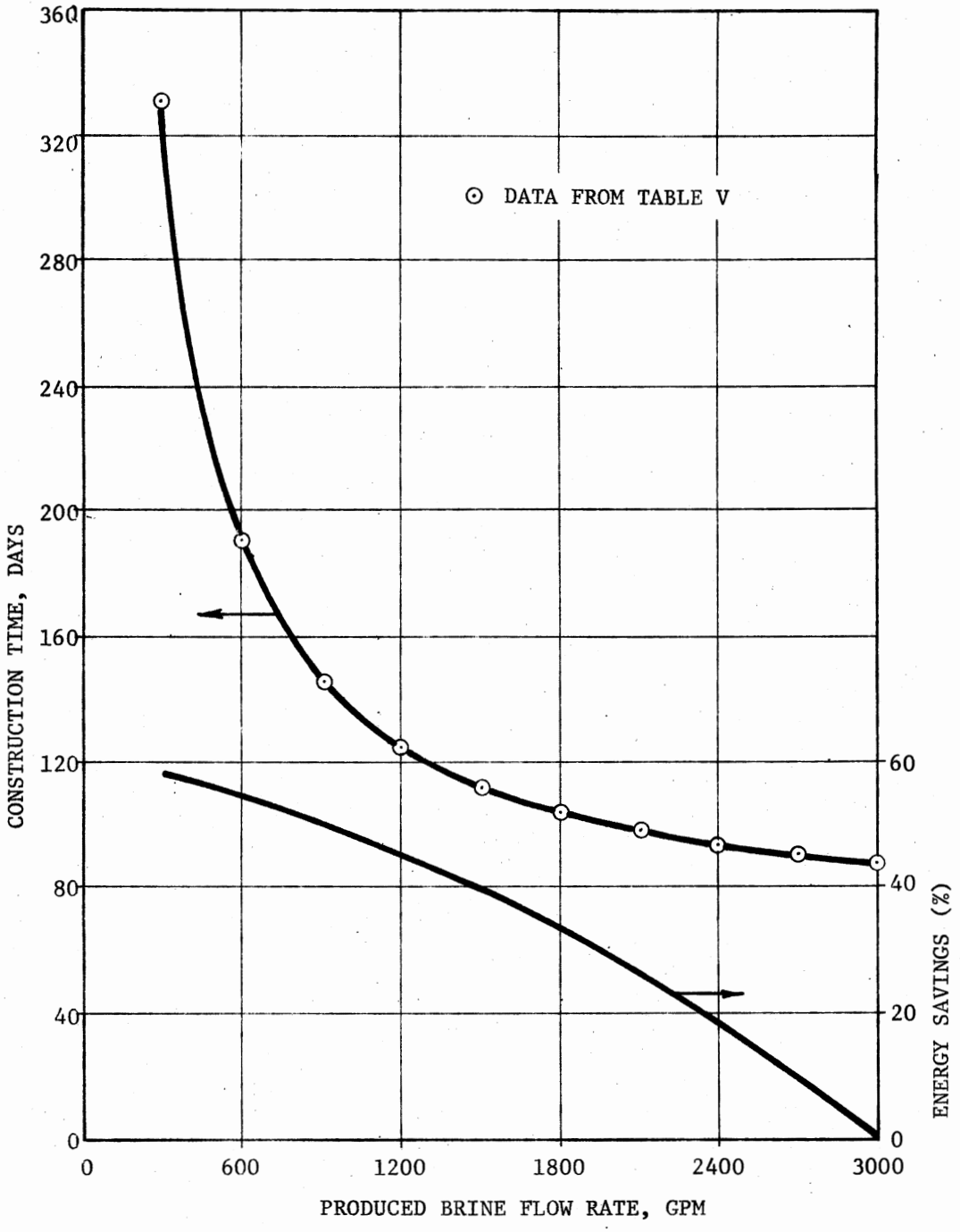

Figure 19. Sump Construction Time and Energy Savings vs. Produced Brine Flow Rate

has a corresponding energy savings of approximately 58 percent of that required for the baseline case.

Also, in order to obtain a minimum energy savings of five percent over baseline case requirements, the produced brine flow rate should not exceed 2,850 gpm. This will result in two days construction time more than for the baseline case.

Figure 20 shows a plot for cavern construction time and energy savings versus produced brine flow rate. At 300 gpm the construction time of 2,241 days has a corresponding energy savings of approximately 31 percent as compared to the baseline case. A five percent energy savings for cavern construction would require that the flow rate not exceed 2,750 gpm which would require a minimum of 22 days more than for the baseline case.

Mathematical Formulation of Problem

The research objective seeks to specify the produced brine flow rate in order to minimize energy consumed during construction and minimize the time of construction. The energy consumed and the time of construction will therefore be expressed in terms of the flow rate.

Energy Consumed vs. Flow Rate. Equation 4-25 was programmed to compute the accumulative energy consumed for each of the nine simulation runs and the baseline case. Figures 21 and 22 illustrate the results. Curve fitting the data points gives the following expression for energy consumed during sump construction as a function of produced brine flow rate.

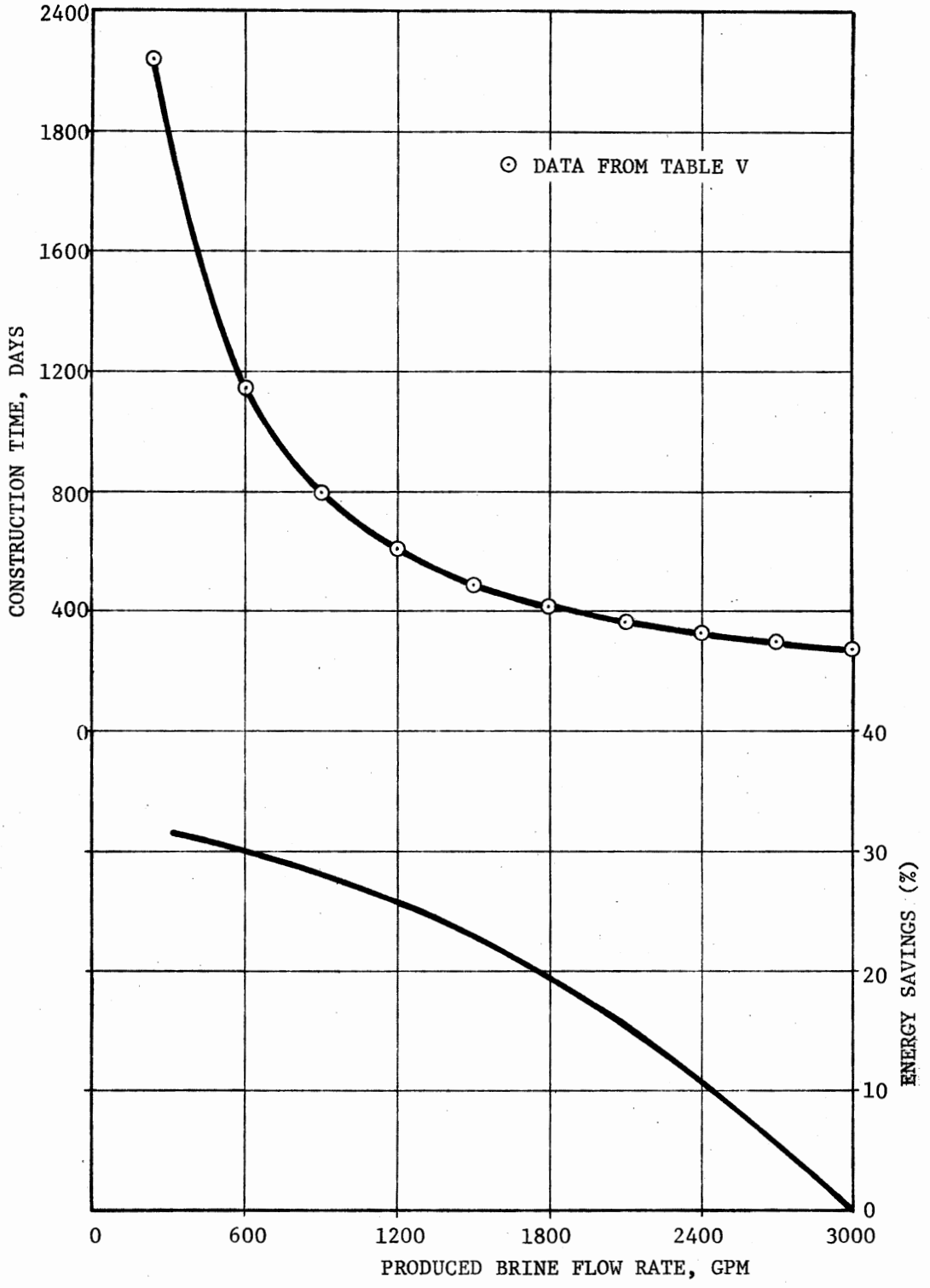

Figure 20. Cavern Construction Time and Energy Savings vs. Produced Brine Flow Rate

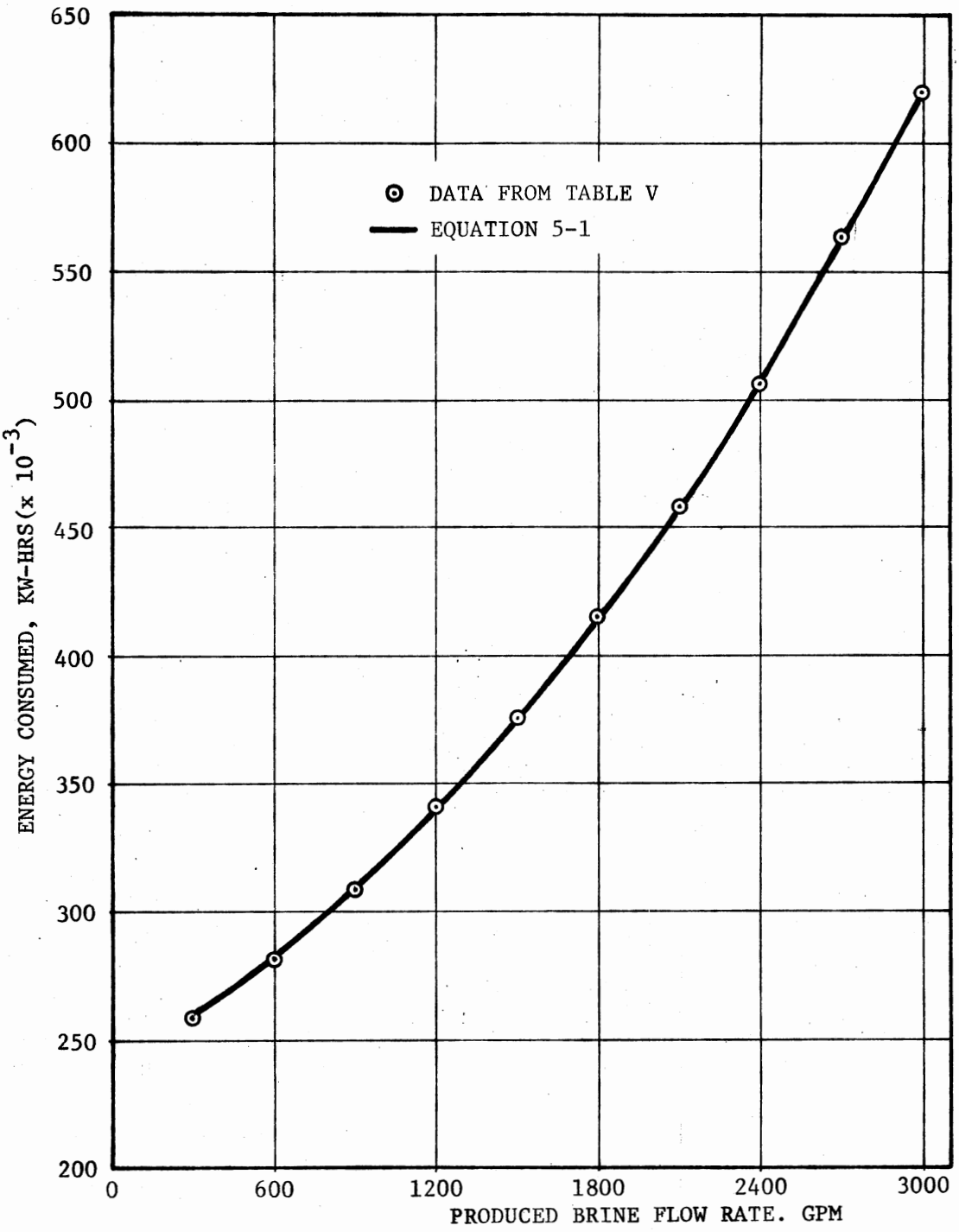

Figure 21. Energy Consumed vs. Produced Brine Flow Rate for Sump Construction

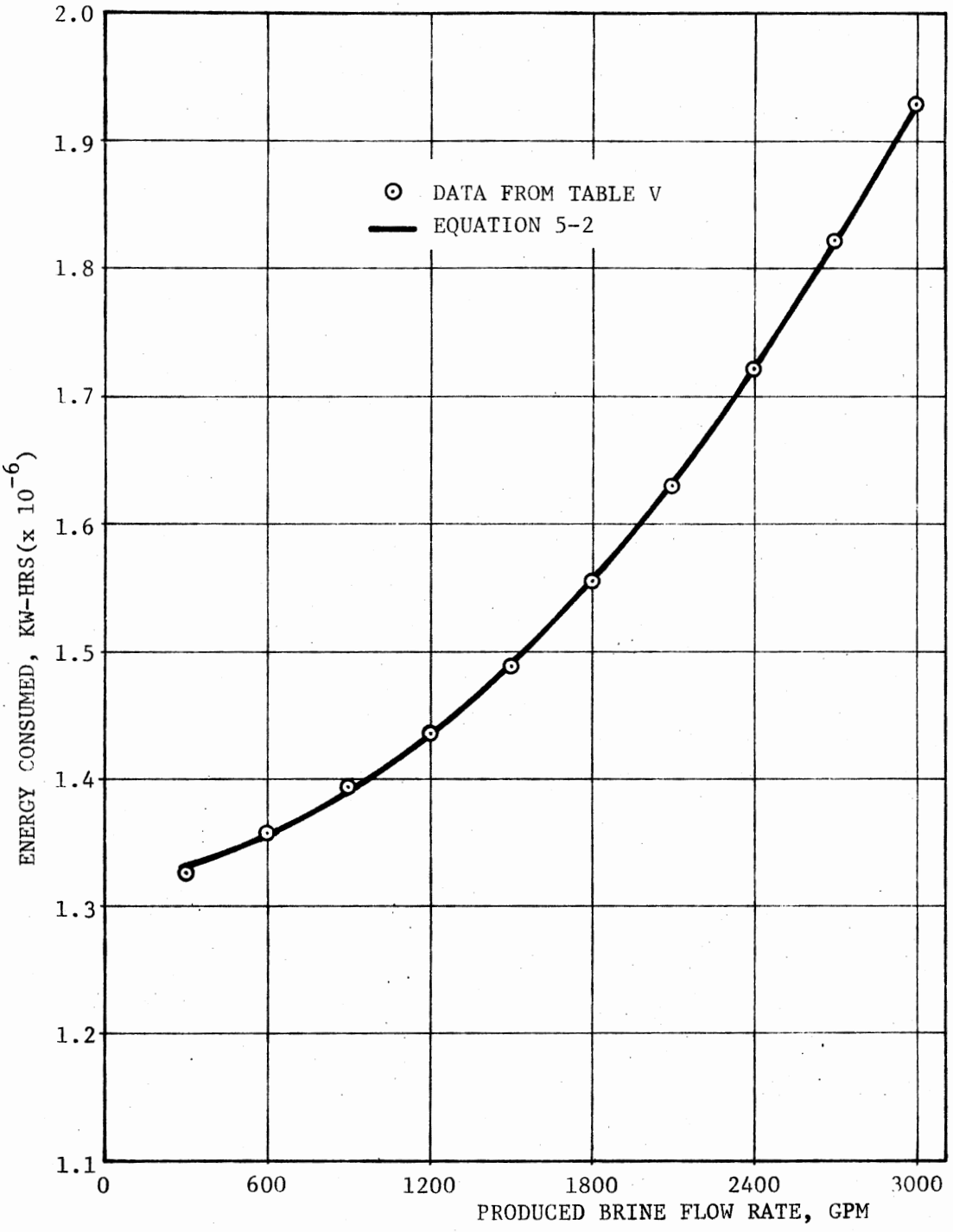

Figure 22. Energy Consumed vs. Produced Brine Flow Rate for Cavern Construction

$$\text{Energy consumed during sump construction} = E_s(Q) = 2.408301813 \times 10^{5} + 5.294201120 \times 10^{1}\, Q + 2.453884584 \times 10^{-2}\, Q^2 \quad (5\text{-}1)$$

The expression for energy consumed during cavern construction as a function of produced brine flow rate is given by Equation 5-2.

$$\text{Energy consumed during cavern construction} = E_c(Q) = 1.318749709 \times 10^{6} + 2.428126310 \times 10^{1}\, Q + 5.972554350 \times 10^{-2}\, Q^2 \quad (5\text{-}2)$$

Construction Time vs. Flow Rate. Equations were also developed to fit the data in Table V concerning construction time versus produced brine flow rate. Figure 23 shows a plot of the data points generated by simulated construction of the sump. Also plotted in the same figures is the following equation that was fitted to the data:

$$\text{Time for construction of sump} = T_s(Q) = \frac{77{,}600}{Q} + 61.666\ldots \quad (5\text{-}3)$$

The equation developed to fit the data for cavern construction is

$$\text{Time for construction of cavern} = T_c(Q) = \frac{665{,}600}{Q} + 48.6667 \quad (5\text{-}4)$$

Simulated construction data and Equation 5-4 are plotted in Figure 24.

Value Theory. The energy consumed and the construction time are now combined mathematically to form a multifactor function. The factors represent dissimilar entities, i.e., the dimensional units of energy and construction time are kw-hrs and days respectively.

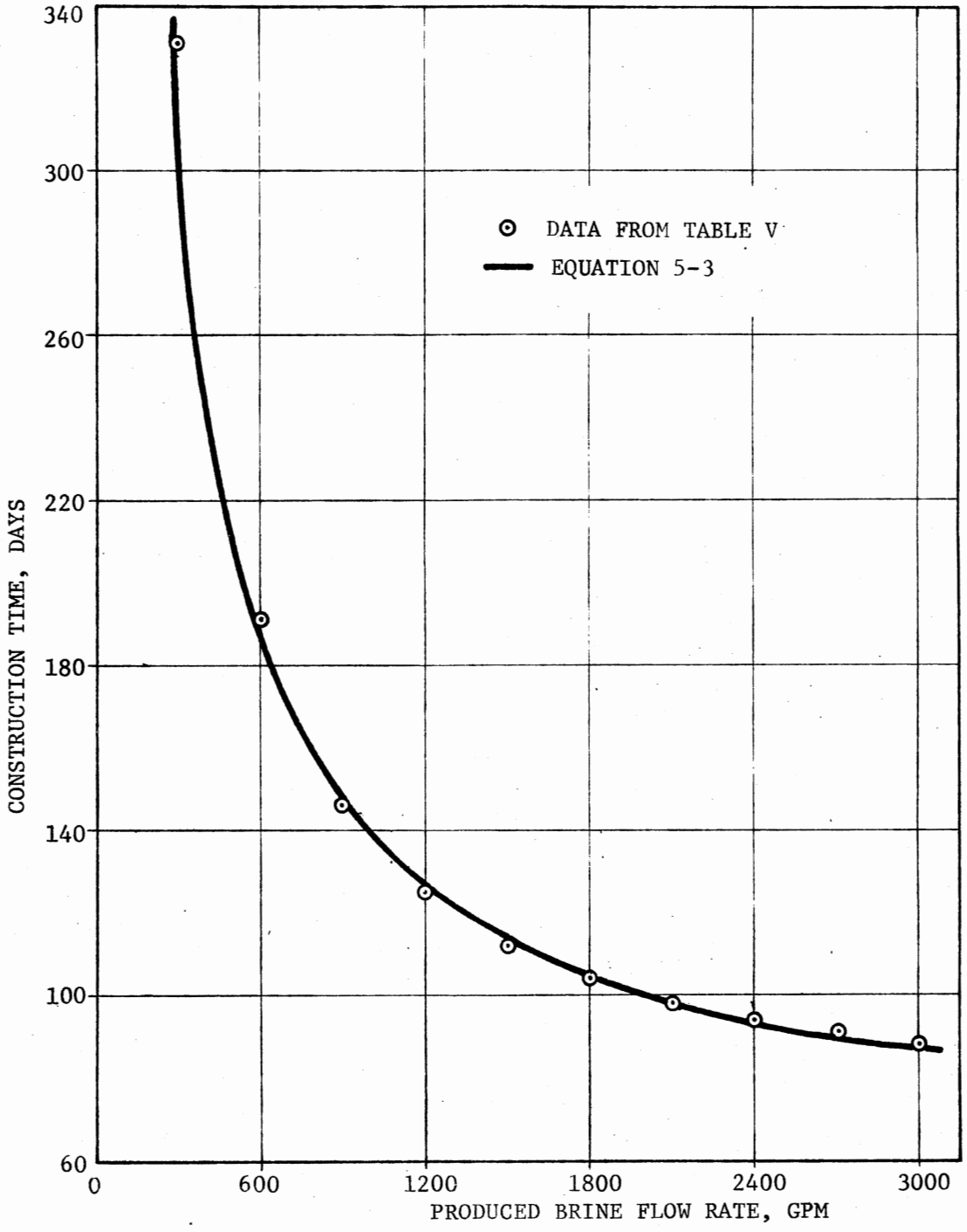

Figure 23. Construction Time vs. Produced Brine Flow Rate for Sump Construction

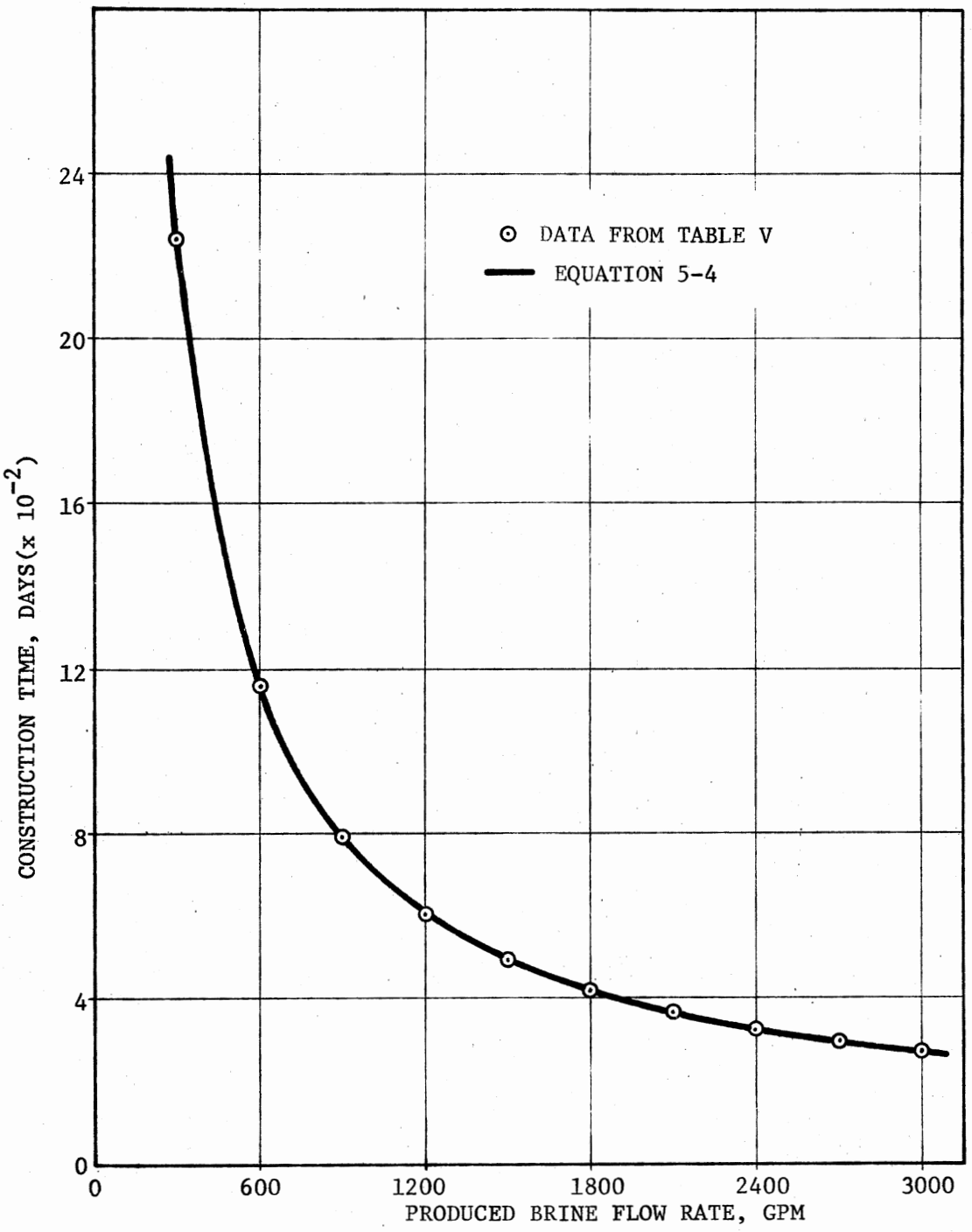

Figure 24. Construction Time vs. Produced Brine Flow Rate for Cavern Construction

Value theory as explained by Gottfried and Weisman (10) on pages 7-9 will be used to set up the mathematical formulation of the problem. The resulting function expressing the research objective is called the value function and is given by

$$\text{Minimize } V = w_1 V_1 + w_2 V_2 \tag{5-5}$$

where V is the overall value, V_1 is the energy consumption value, V_2 is the construction time value, and w_1 and w_2 are weighting factors used to express the relative importance of the two factors. A separate value function is written for sump construction and cavern construction.

For the energy consumed and for the construction time, separate numerical scales are set up going from 0 to 1. For energy consumed during sump construction, a value of 0 is assigned to 258,330 kw-hrs (refer to Table V) occurring at the produced flow rate of 300 gpm, and a value of 1 is assigned to 620,891 kw-hrs occurring at 3,000 gpm. Any other value of energy consumed will have a fractional value between 0 and 1 according to the following value factor equation:

$$(V_1)_s = \frac{E_s(Q) - 258,330}{620,891 - 258,330}$$

$$= \frac{1}{362,561}\,(E_s(Q) - 258,330), \quad 300 \leq Q \leq 3000 \tag{5-6}$$

where $E_s(Q)$ is defined by Equation 5-1. Note that as $E_s(Q)$ increases, $(V_1)_s$ increases in value.

Likewise for cavern construction, the companion value factor equation for energy consumption is

$$(V_1)_c = \frac{1}{603,403}(E_c(Q) - 1,326,543), \quad 300 \leq Q \leq 3000. \tag{5-7}$$

Value factor equations for the construction time for the sump and cavern were developed resulting in the following two expressions:

$$(V_2)_s = \frac{T_s(Q) - 88}{331 - 88}$$

$$= \frac{1}{243}[T_s(Q) - 88], \quad 300 \leq Q \leq 3000, \tag{5-8}$$

and

$$(V_2)_c = \frac{T_c(Q) - 268}{2241 - 268}$$

$$= \frac{1}{1973}[T_c(Q) - 268], \quad 300 \leq Q \leq 3000, \tag{5-9}$$

where $T_s(Q)$ and $T_c(Q)$ are defined as the construction times for sump and cavern construction in terms of the produced brine flow rate Q and are given by Equations 5-3 and 5-4, respectively. As $T_s(Q)$ and $T_c(Q)$ decrease, $(V_2)_s$ and $(V_2)_c$ decrease in numerical value.

By combining Equations 5-1 and 5-6 and Equations 5-3 and 5-8, then substituting into Equation 5-5 results in the value function for sump construction as given by

$$\text{Minimize } V_s = w_1\left[\frac{1}{362,561}(-17,499.8187 + 52.9420112\ Q + 2.453884584 \times 10^{-2}\ Q^2)\right] + w_2\left[\frac{1}{243}\left(\frac{77,600}{Q} - 26.3333\right)\right], \quad 300 \leq Q \leq 3000. \tag{5-10}$$

Figure 25 illustrates Equation 5-10 evaluated for various values of w_2/w_1.

The corresponding value function for cavern construction is

$$\text{Minimize } V_c = w_1\left[\frac{1}{603,403}(-7793.291 + 24.2812631\ Q + 5.972554350 \times 10^{-2}\ Q^2)\right] + w_2\left[\frac{1}{1973}\left(\frac{665,600}{Q} - 219.3333\right)\right], \quad 300 \leq Q \leq 3000. \tag{5-11}$$

Figure 26 illustrates Equation 5-11 evaluated for selected values of w_2/w_1.

Optimization of Value Functions

Fundamental optimization was used to solve for the extreme value in Equations 5-10 and 5-11.

Sump Construction. Equation 5-10 may be written as

$$\text{Minimize } V_s = w_1\ 6.768197859 \times 10^{-8}\ Q^2 + w_1\ 1.460223554 \times 10^{-4}\ Q + w_2\ \frac{319.3415638}{Q} + \text{constant} \tag{5-12}$$

The extreme point of this function can be obtained by differentiating V_s with respect to Q, equating the result to zero, and solving for Q_o (the optimal value for the produced brine flow rate). Then Q_o is substituted into Equation 5-10 to obtain $(V_s)_o$.

Setting the first derivative of V_s with respect to Q equal to zero yields

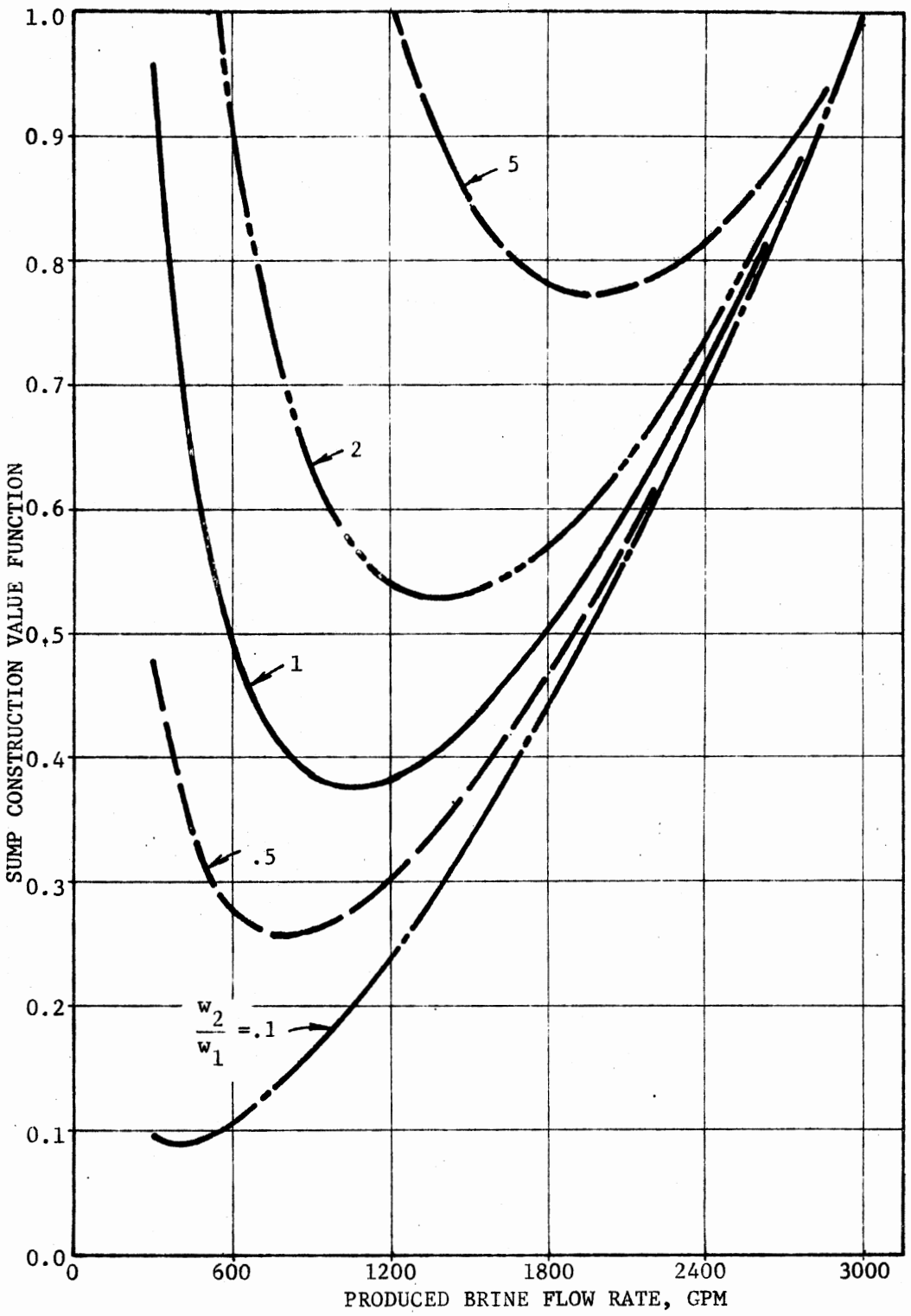

Figure 25. Sump Construction Value Function vs. Produced Brine Flow Rate

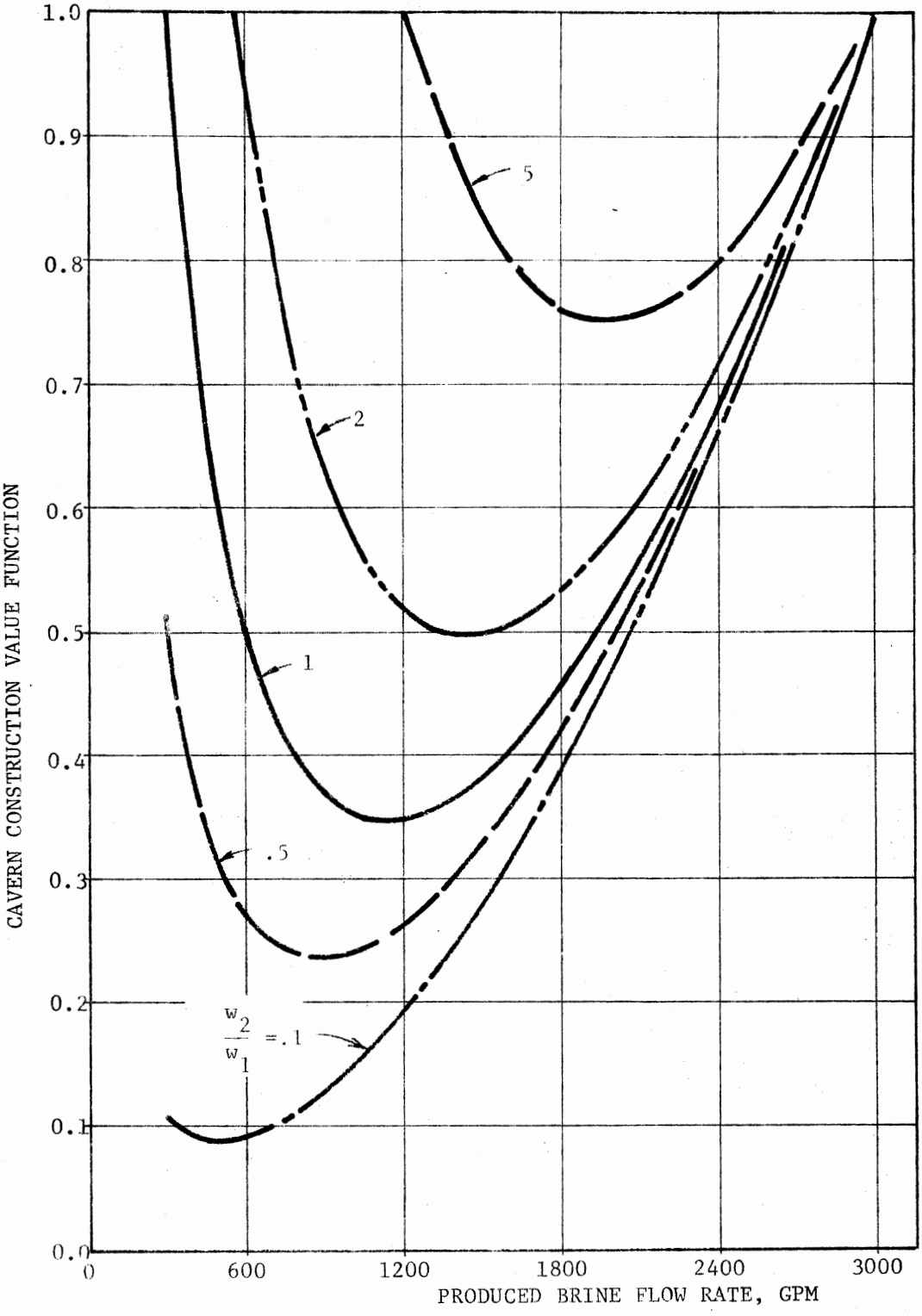

Figure 26. Cavern Construction Value Function vs. Produced Brine Flow Rate

$$\frac{dV_s}{dQ} = 2(6.768197859 \times 10^{-8})\, Q_o + (1.460223554 \times 10^{-4}) - \frac{w_2}{w_1}(319.3415638)\, Q_o^{-2} = 0 \qquad (5\text{-}13)$$

Multiplying through by Q_o^2 and regrouping terms yields

$$Q_o^3 + a\, Q_o^2 + c = 0 \qquad (5\text{-}14a)$$

where:

$$a = 1078.736194 \qquad (5\text{-}14b)$$

$$c = -1.359132892 \times 10^9 \left(\frac{w_2}{w_1}\right). \qquad (5\text{-}14c)$$

The technique used to solve Equation 5-14a for Q_o is taken from Newman (12) pages 197-199 and is the subject of Appendix B.

Let

$$p = -\frac{a^2}{9} = 1.292968640 \times 10^5, \qquad (5\text{-}15a)$$

and

$$q = \frac{a^3}{27} + \frac{c}{2} = 4.649240234 \times 10^7 - 1.179566446 \times 10^9\left(\frac{w_2}{w_1}\right). \qquad (5\text{-}15b)$$

For approximately $7.88296454 \times 10^{-2} \leq w_2/w_1 < 2.371751149 \times 10^{-11}$, $q^2 + p^3 \geq 0$, and the optimal value of the produced brine flow rate Q_o is given by

$$Q_o = u + v - \frac{a}{3} \tag{5-16a}$$

where:

$$u = \sqrt[3]{-q + \sqrt{q^2 + p^3}} \tag{5-16b}$$

$$v = \sqrt[3]{-q - \sqrt{q^2 + p^3}} \tag{5-16c}$$

For other values of w_2/w_1 the optimal produced brine flow rate is given by

$$Q_o = 2\sqrt{-p}\cos\frac{\varphi}{3} \tag{5-17a}$$

where φ is in degrees and determined by

$$\varphi = \cos^{-1}\frac{-q}{\sqrt{-p^3}}. \tag{5-17b}$$

Cavern Construction. For cavern construction the companion equation 5-14a is given by

$$Q_o^3 + a\,Q_o^2 + c = 0 \tag{5-18a}$$

where:

$$a = 203.2736889 \tag{5-18b}$$

$$c = -1.704133394 \times 10^9\left(\frac{w_2}{w_1}\right). \tag{5-18c}$$

Furthermore,

$$p = -4.591132512 \times 10^3, \tag{5- 9a}$$

and

$$q = 3.110854807 \times 10^{5} - 8.520666970 \times 10^{8}\left(\frac{w_2}{w_1}\right). \qquad (5\text{-}19b)$$

For approximately $w_2/w_1 \geq 7.3 \times 10^{-4}$, $q^2 + p^3 \geq 0$, and Equation 5-16a, 5-16b, and 5-16c are used to solve for the optimal value of the produced brine flow rate Q_o. For values of w_2/w_1 between zero and less than approximately 7.3×10^{-4}, $q^2 + p^3 < 0$, and Equations 5-17a and 5-17b are used to solve for Q_o.

In Table VI optimal values of the produced brine flow rate for sump construction and cavern construction are listed for various values of w_2/w_1. For sump construction the maximum value of w_2/w_1 that results in Q_o equal to 3,000 gpm is approximately 15.5. Likewise for cavern construction w_2/w_1 equal to 17 yields Q_o equal to approximately 3,000 gpm.

A research objective was to determine operating conditions which will result in a minimum of five percent savings in energy compared to energy requirements when operating at 3,000 gpm. Earlier in this chapter it was determined that to meet this requirement the produced brine flow rate for sump construction and cavern construction should not exceed 2,850 gpm and 2,750 gpm, respectively. Therefore, for sump and cavern construction the values for w_2/w_1 should not exceed the approximate values of 13.5 and 13.

Sensitivity Analysis and Managerial Operating Range

Sensitivity analysis of a value function was performed to determine how deviations from an optimal solution affects the function value. The managerial operating range for a decision variable, in this case the

TABLE VI

OPTIMAL VALUES OF PRODUCED BRINE FLOW RATE VS. W2/W1

$\frac{W_2}{W_1}$	Optimal value of produced brine flow rate, gpm	
	Sump construction*	Cavern construction*
0.1	399	494
0.2	540	637
0.3	641	737
0.4	724	817
0.5	794	885
0.6	855	944
0.7	911	997
0.8	962	1045
0.9	1009	1089
1	1052	1130
2	1384	1440
3	1620	1658
4	1808	1831
5	1968	1977
6	2108	2105
7	2233	2219
8	2347	2323
9	2452	2419
10	2550	2507
11	2641	2590
12	2727	2669
13	2809	2743
14	2886	2812
15	2960	2879
16	3031	2944
17	--	3005

*Table entries rounded off to nearest whole number.

produced brine flow rate, is the range of values for that variable for which the resulting numerical value of the value function is maintained within a predetermined allowable deviation.

This subsection develops the sensitivity analysis and the managerial operating range for sump and cavern construction. The techniques employed are explained by Abouel-Nour (12) on pages 68-70 and by Shamblin and Stevens (13) on pages 225-233.

Sensitivity Analysis for Sump Construction. A sensitivity measure is denoted by the parameter k and defined as

$$k = \frac{TVV_s}{(TVV_s)_o}, \quad k \geq 1 \tag{5-20}$$

where TVV_s is the total variable value of the value function for sump construction, i.e., (Equation 5-12) with the constant term deleted. Only terms containing Q are considered to be under control of the manager. $(TVV_s)_o$ is the minimum value of TVV_s.

An error term w is defined as a deviation of the produced brine flow rate from its optimal value, or

$$Q = w\,Q_o, \quad w > 0 \tag{5-21}$$

The corresponding $(TVV_s)_w$ is

$$(TVV_s)_w = (6.768197859 \times 10^{-8}\, Q_o^2)\, w^2 + (1.460223554 \times 10^{-4}\, Q_o)\, w \pm (w_2/w_1)\left(\frac{319.3415638}{Q_o}\right)\frac{1}{w}, \tag{5-22}$$

and the resulting sensitivity expression is

$$\frac{(TVV_s)_w}{(TVV_s)_o} = k = A_o w^2 + B_o w + C_o \frac{1}{w}, \tag{5-23a}$$

where:

$$A_o = 6.768197859 \times 10^{-8} \, Q_o^2/(TVV_s)_o \qquad (5\text{-}23b)$$

$$B_o = 1.460223554 \times 10^{-4} \, Q_o/(TVV_s)_o \qquad (5\text{-}23c)$$

$$C_o = (w_2/w_1)\left(\frac{319.3415638}{Q_o}\right)/(TVV_s)_o \qquad (5\text{-}23d)$$

To illustrate the relationship between k and w, Table VII was constructed using Equation 5-23a with w_2/w_1 equal to 1.

TABLE VII

SENSITIVITY OF THE PRODUCED BRINE FLOW RATE ON THE VALUE FUNCTION RATIO k FOR SUMP CONSTRUCTION

w	$k = \frac{(TVV_s)_w}{(TVV_s)_o}$	w	$k = \frac{(TVV_s)_w}{(TVV_s)_o}$
0.5	1.3204	1.1	1.0066
0.6	1.1746	1.2	1.0246
0.7	1.0860	1.3	1.0522
0.8	1.0342	1.4	1.0877
0.9	1.0077	1.5	1.1303
1.0	1.0000		

Therefore, if the produced brine flow rate deviates 30 percent (w = 0.7) below its optimal value, there will be an 8.6 percent increase in the minimum value of the value function. Likewise, for a

flow rate say 40 percent above the optimal value, an increase in the minimum value of the value function of 8.77 percent will result.

Managerial Operating Range for Sump Construction. From Equation 3-23a, w is solved for in terms of k which results in the cubic equation

$$w^3 + \frac{B_o}{A_o} w^2 - \frac{k_w}{A_o} + \frac{C_o}{A_o} = 0. \tag{5-24}$$

Using the technique of Appendix B, Equation 5-24 can be reduced to

$$x^3 + 3px + 2q = 0 \tag{5-25}$$

by using the substitution

$$w = x - \frac{B_o}{3A_o}. \tag{5-26}$$

The variables p and q in Equation 5-25 are defined as follows:

$$p = \frac{-4.924993923 \times 10^6 k(TVV_s)_o - 5.171899739 \times 10^5}{Q_o^2} \tag{5-27}$$

$$q = \frac{3.719419347 \times 10^8 + 5.312782132 \times 10^9 k(TVV_s)_o}{Q_o^3} + \frac{2.359132892 \times 10^9 (w_2/w_1)}{Q_o^3} \tag{5-28}$$

In this research the sensitivity parameter k was limited to values between 1.0 and 1.10, or TVV_s was allowed to deviate from its optimal value by up to ten percent. For sump construction

$$q^2 + p^3 \leq 0 \tag{5-29}$$

where the ratio of weighting factors w_2/w_1 was limited to values between 0.1 and 15.5.

Solution of Equation 5-25 yields three real and different roots, one of which is negative. The positive roots, say x_1 and x_2, are substituted into Equation 5-26 resulting in a w_1 and w_2. Final substitution of these values of w into Equation 5-21 yields the upper and lower limits for the produced brine flow rate Q that will maintain TVV_s within a predetermined allowable deviation from its optimal value. The managerial operating range (MOR) is defined by the limits on Q.

The MOR for the produced brine flow rate is mathematically defined by

$$Q_{\substack{\text{upper}\\\text{limit}}} = Q_o \left(2\sqrt{-p} \cos \frac{\varphi}{3} - \frac{B_o}{3A_o} \right) \tag{5-30}$$

$$Q_{\substack{\text{lower}\\\text{limit}}} = Q_o \left(-2\sqrt{-p} \cos \left(\frac{\varphi}{3} + 60^\circ \right) \right) \tag{5-31}$$

where

$$\varphi = \cos^{-1} \frac{-q}{\sqrt{-p^3}}. \tag{5-32}$$

Table X of Appendix C lists the MOR for the produced brine flow rate over a range of values for k and w_2/w_1. The results show that when w_2/w_1 is equal to 1, Q may vary between 803 and 1,361 gpm when TVV_s deviates from its optimal value by five percent (k = 1.050) and between 716 and 1,505 gpm when a ten-percent deviation is allowed. Table X also illustrates that for higher values of w_2/w_1, the upper allowable limit of Q exceeds 3,000 gpm--a limit of investigation placed on this study.

In addition, for some values of w_2/w_1 and k the upper limit for Q is greater than 2,850 gpm and, thus, violates the constraint that must not be exceeded in order to obtain a five-percent energy savings. For the case of w_2/w_1 equal to ten and k equal to 1.020 the MOR in Table X is given by $2,175 \leq MOR \leq 2,971$. However, by taking the constraint into account reduces the MOR to $2,175 \leq Q \leq 2,850$.

Figure 27 illustrates the MOR concept for k = 1.050 and k = 1.100 when w_2/w_1 equls one.

Sensitivity Analysis for Cavern Construction. For cavern construction, the total variable value of the value function (TVV_c) as a function of the error term w (refer to Equation 5-22) is given by

$$(TVV_c)_w = (9.898118422 \times 10^{-8} Q_o^2)w^2 + (4.024054090 \times 10^{-5} Q_o)w + (w_2/w_1)\left(\frac{337.3542828}{Q_o}\right)\frac{1}{w}, \quad (5\text{-}33)$$

and the sensitivity expression is given by

$$\frac{(TVV_c)_w}{(TVV_c)_o} = k = A_o w^2 + B_o w + C_o \frac{1}{w} \quad (5\text{-}34a)$$

where:

$$A_o = 9.898118422 \times 10^{-8} Q_o^2/(TVV_c)_o \quad (5\text{-}34b)$$

$$B_o = 4.024054090 \times 10^{-5} Q_o/(TVV_c)_o \quad (5\text{-}34c)$$

$$C_o = (w_2/w_1)\left(\frac{337.3542828}{Q_o}\right)/(TVV_c)_o \quad (5\text{-}34d)$$

Table VIII lists the values of w for various values of k when w_2/w_1 is set equal to 1.

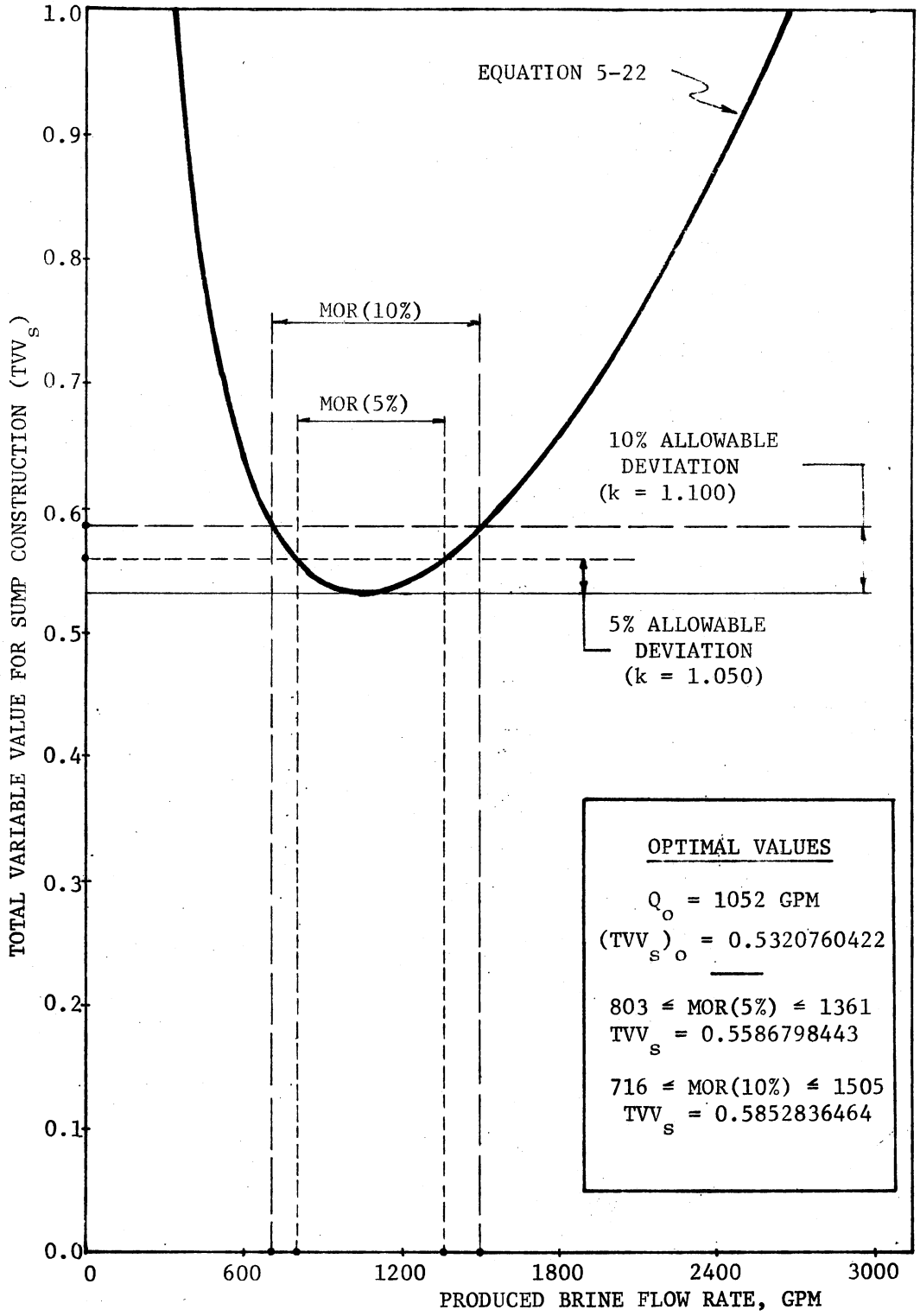

Figure 27. Total Variable Value vs. Produced Brine Flow Rate for Sump Construction

TABLE VIII

SENSITIVITY OF THE PRODUCED BRINE FLOW RATE ON THE VALUE FUNCTION RATIO k FOR CAVERN CONSTRUCTION

w	$k = \frac{(TVV_c)_w}{(TVV_c)_o}$	w	$k = \frac{(TVV_c)_w}{(TVV_c)_o}$
0.5	1.3844	1.1	1.0085
0.6	1.2122	1.2	1.0319
0.7	1.1058	1.3	1.0681
0.8	1.0425	1.4	1.1155
0.9	1.0097	1.5	1.1730
1.0	1.0000		

Managerial Operating Range for Cavern Construction. Solving Equation 5-34a for w in terms of k yields

$$w^3 + \frac{B_o}{A_o} w^2 + \frac{k}{A_o} w + \frac{C_o}{A_o} = 0. \qquad (5\text{-}35)$$

Using Equations 5-34 b-d, Equation 5-35, and Appendix B, the following expressions for p and q were developed:

$$p = \frac{-3.367643417 \times 10^6 k(TVV_c)_o - 1.836453005 \times 10^4}{Q_o^2} \qquad (5\text{-}36)$$

$$q = \frac{2.488683845 \times 10^6 + 6.845533003 \times 10^8 k(TVV_c)_o}{Q_o^3} + \frac{1.704133394 \times 10^9 (w_2/w_1)}{Q_o^3} \qquad (5\text{-}37)$$

The MOR for the produced brine flow rate is determined by substituting Equations 5-36 and 5-37 into Equations 5-30, 5-31, and 5-32. Table XI of Appendix C lists the MOR for the flow rate over a range of values for k and w_2/w_1. For some values of w_2/w_1 the upper limit on the flow rate exceeds the 2,750 gpm constraint previously set in order to conserve energy. For the case of w_2/w_1 equal to ten and k equal to 1.010 the MOR from Table XI is given by $2,259 \leq \text{MOR} \leq 2,773$. Taking the constraint into account reduces the operating range to $2,259 \leq \text{MOR} \leq 2,750$.

Figure 28 illustrates the MOR concept for k = 1.050 and k = 1.100 when w_2/w_1 equals one.

The steps leading to an optimal produced brine flow rate with an associated managerial operating range are outlined in an algorithm presented in Appendix D.

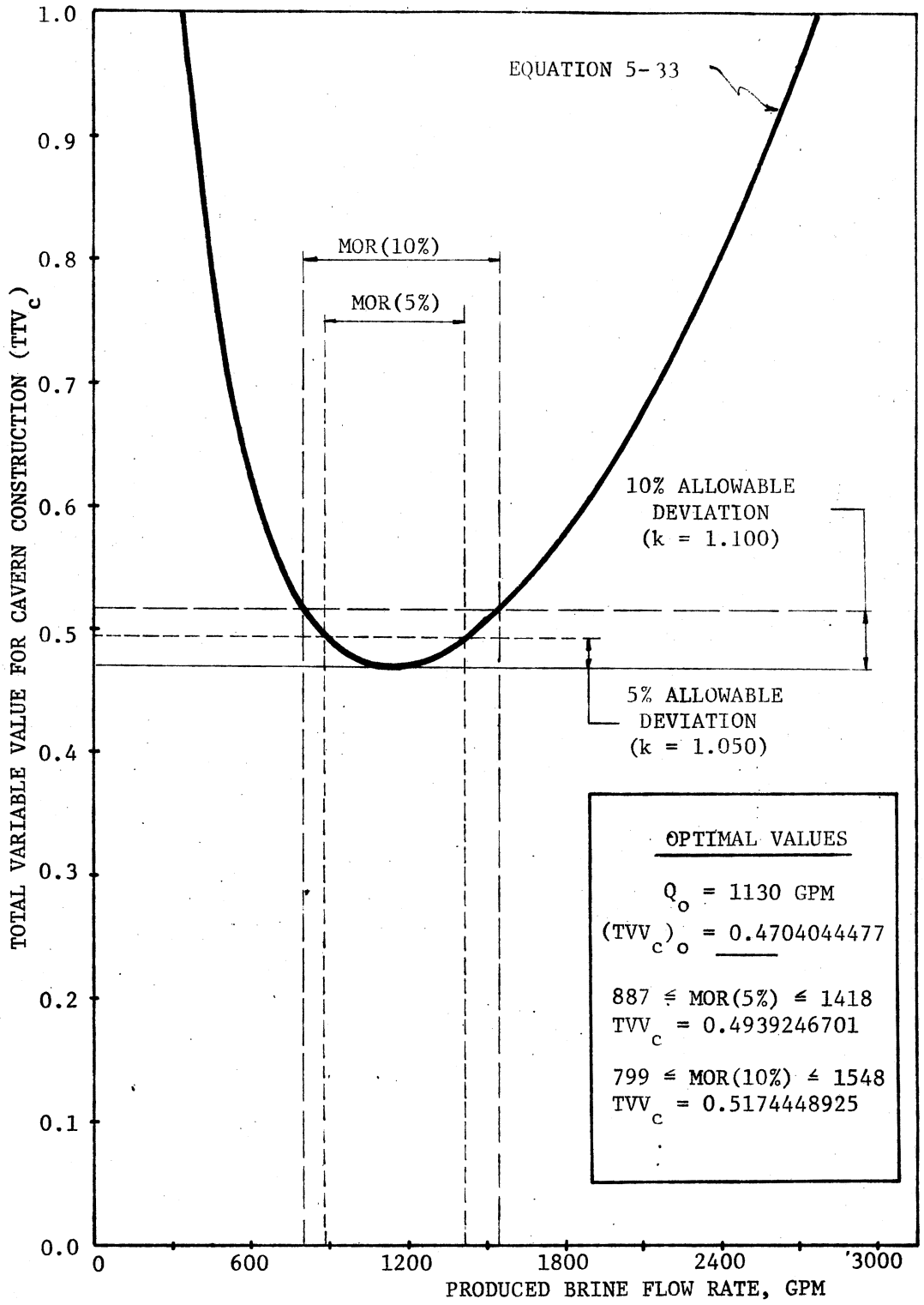

Figure 28. Total Variable Value vs. Produced Brine Flow Rate for Cavern Construction

CHAPTER VI

SUMMARY, CONCLUSIONS, AND RECOMMENDATIONS

In summary, this research establishes a mathematical model suitable for studying a proposed or actual solution mining cavern construction system. Theory that described the dissolution mechanisms of dome salt existed and was integrated into this study. Fluid mechanics theory was developed to relate the resulting flow of brine from the cavern during construction to energy consumed.

The research objective was composed of two conflicting factors and one constraint. It was desired to specify a flow rate through the cavern that would minimize total energy consumed but also minimize the total construction time. The constraint specified that a savings of five percent of the total energy consumed must be realized for both sump and cavern construction when compared to a baseline case where total pumping capacity was used at all times.

A test construction system was modelled, and simulated construction of a 4,000,000 barrel cavern with a 400,000 barrel sump was studied. Value theory was used to mathematically formulate the multi-factor research objectives for the system.

For construction of the sump using input parameters listed in Tables I and II, the conclusions are:

1. The baseline case showed that the sump could be constructed in 88 days using a flow rate of 3,000 gpm. To reduce energy

consumption by five percent, the flow rate should be reduced to 2,850 gpm which would add another two days to the construction time.

2. The relative weighting of the two research objective factors w_2/w_1 could range in value from 0 to approximately 13.5. Higher values would violate the five percent energy savings constraint.
3. When w_2/w_1 equals 1, the optimal produced brine flow rate was determined to be 1,052 gpm. Table VI lists optimal flow rates for other relative weightings.
4. For the optimal condition mentioned in 3 above, the managerial operating range for the flow rate is from 803 gpm to 1,361 gpm when the research objective was allowed a maximum five percent deviation from its optimal value. Table X lists operating ranges for the flow rate for various other situations.

For construction of the cavern using input parameters listed in Tables I and III, the conclusions are:

1. The baseline case showed that the cavern could be constructed in 268 days using a flow rate of 3,000 gpm. By reducing the flow rate to 2,750 gpm, the five percent reduction in energy consumption could be obtained which would prolong construction by 22 days.
2. The range on w_2/w_1 for cavern construction was found to be between 0 and approximately 13 before the energy savings constraint was violated.
3. When w_2/w_1 equals 1, the optimal value for the produced

brine flow rate was determined to be 1,130 gpm. Table VI lists optimal flow rates for other relative weightings.

4. For the optimal condition mentioned in 3 above, the managerial operating range for the flow rate is from 887 gpm to 1,418 gpm for an allowable five percent deviation from the optimal value of the research objective.

Other general conclusions drawn from this research are:

1. As the relative importance of constructing a sump and cavern in minimum time increases, the produced brine flow rate MOR increases for a given allowable deviation from the optimal objective value.
2. For a given value of w_2/w_1, as the allowable deviation from the optimal objective value increases the MOR for the flow rate increases.

Recommendations to improve upon and extend this initial research effort are listed below.

1. Apply single variable search techniques to find the extreme points for the cubic equations used for 1) the value functions and 2) the determination of the managerial operating ranges for this study. The goal would be to reduce any roundoff error.
2. Develop methods to handle multivariable, multifactor research objectives. Suggestions for other variables to consider that are related to energy consumption are 1) pipeline and casing diameters, 2) depth at which the sump and cavern are constructed, 3) positioning and relocation of the casings in the cavern during

construction, and 4) cavern height vs. diameter ratio for given cavern volumes. Other factors to consider could include total investment cost and total operating cost.

3. Modify Saberian's computer program to simulate sump construction, store the necessary data, then simulate cavern construction without restarting the program for cavern construction. Present procedures require separate starts for each run.

A SELECTED BIBLIOGRAPHY

(1) Oklahoma Energy Conservation Plan - A Summary. Oklahoma City: Oklahoma Department of Energy, n.d., p. 1.

(2) Saberian, Ahmad. "Numerical Simulation of Development of Solution-Mined Salt Cavities." A Solution Mining Research Institute Project-Progress Report, August, 1974. Austin, Texas: Petroleum Engineering Department, University of Texas at Austin (Research funded by SMRI).

(3) First Symposium on Salt, (1 Vol.), 1963.
Second Symposium on Salt, (2 Vols.), 1966.
Third Symposium on Salt, (2 Vols.), 1970.
Fourth Symposium on Salt, (2 Vols.), 1974.
Cleveland, Ohio: Northern Ohio Geological Society, Inc.

(4) Jessen, F. W. "Total Solution Mechanism." Society of Mining Engineers, AIME Transactions, Vol. 250 (December, 1971), pp. 298-304.

(5) Remson, D. R., O. D. Dommers, and F. W. Jessen. "Techniques for Developing Predetermined Shaped Cavities in Solution Mining." Second Symposium on Salt. Cleveland, Ohio: Northwestern Ohio Geological Society (1966), pp. 297-310.

(6) Pottier, Michel, and Bernard Esteve. "Simulation of Gas Storage Cavity Creation by Numerical Methods." Fourth Symposium on Salt. Cleveland, Ohio: Northwestern Ohio Geological Society (1974), pp. 291-300.

(7) Meister, S., et al. "Numerical Simulation of the Leaching Processes." EKEP - SYNOPSIS 75 013 (Note on translated abstract--complete article was published in Compendium 74/75).

(8) Snow, Richard H., and Davy S. Chang. Prediction of Cavity Growth by Solution of Salt Around Boreholes. Report No. IITRI C6313-14, IIT Research Institute, Chicago, Ill., 1975.

(9) Brenkert, Karl, Jr. Elementary Theoretical Fluid Mechanics, 2nd ed. New York: John Wiley & Sons, Inc., 1960.

(10) Gottfried, Bryon S., and Joel Weisman. Introduction to Optimization Theory, 1st ed. Englewood Cliffs, New Jersey: Prentice-Hall, 1973.

(11) **Abouel-Nour**, Abdel-Razek A. "Sensitivity Analysis of the Decision Models." (Unpub. Ph.D. dissertation, Oklahoma State University, 1967.)

(12) **Newman**, James R. The Universal Encyclopedia of Mathematics. (English translation and adaptation copyright, 1964 by George Allen and Unwin, Ltd.), 1st ed. New York: The New American Library of World Literature, Inc., 1965.

(13) **Shamblin**, James E., and G. T. Stevens, Jr. Operations Research, A Fundamental Approach, 1st ed. New York: McGraw-Hill, 1974.

(14) "Flow of Fluids Through Valves, Fittings, and Pipe." Technical Paper No. 410. Chicago, Illinois: Crane Co., 1965, Appendix A.

APPENDIX A

DETERMINATION OF OUTPUT VOLUME TO INPUT VOLUME RATIO

The volume of fluid produced from a cell during leaching will always be less than the volume of fluid entering the cell assuming a constant temperature process. The only exception to this is when the fluid is 100% saturated in which case no dissolution occurs, therefore the volume of fluid entering the cell is equal to the fluid volume leaving the cell. For each gallon of fluid (fresh water or partially saturated brine) entering a cavity cell, an amount of salt will be dissolved from the cavity wall, thus increasing the cell volume. Also, the fluid that is produced by mixing of the dissolved salt with the original gallon of fluid entering the cell has a volume in excess of one gallon. For solution mining of salt dome cavities the chemical dissolution process is such that the increase in volume of new space created (volume of salt dissolved) is always greater than the increase in volume of the leaving fluid. For this reason the volume of fluid leaving a cell is always less than the volume of fluid entering the cell.

A sample calculating will illustrate the phenomenon. The properties of brine used in the calculation are listed in Table IX. A more complete table of properties was developed by the writer as an integral part of this research and is compatible with Saberian's simulation program for brine at $75^{o}F$.

TABLE IX

PROPERTIES OF BRINE AT 75°F

1	2	3	4	5	6	7	8
% Saturation	% Salt by Weight in Brine	Specific Gravity	GPL of Salt in Brine	Gal. Water / Gal. Brine	Lbs. Brine / Gal. Water	Lbs. Salt / Gal. Brine	Lbs. Salt / Gal. Water
0	0.0000	1.00000	0.00000	1.00000	8.345000	0.000000	0.000000
5	1.3157	1.00955	13.28304	0.99627	8.424713	0.110847	0.111262
10	2.6315	1.01910	26.81745	0.99229	8.504430	0.223792	0.225531
15	3.9472	1.02866	40.60322	0.98805	8.584140	0.338834	0.342931
20	5.2629	1.03821	54.64036	0.98357	8.663850	0.455974	0.463591
25	6.5787	1.04776	68.92886	0.97883	8.743570	0.575211	0.587650
30	7.8944	1.05731	83.46872	0.97384	8.823280	0.696546	0.715254
35	9.2101	1.06687	98.25995	0.96861	8.902990	0.819979	0.846556
40	10.5259	1.07657	113.31869	0.96325	8.983990	0.945645	0.981720
45	11.8416	1.08640	128.64733	0.95775	9.066000	1.073562	1.120918
50	13.1574	1.09634	144.24932	0.95209	9.148950	1.203761	1.264335
55	14.4731	1.10639	160.12909	0.94626	9.232840	1.336277	1.412164
60	15.7888	1.11656	176.29106	0.94026	9.317660	1.471149	1.564612
65	17.1046	1.12683	192.73965	0.93409	9.403410	1.608412	1.721900
70	18.4203	1.13722	209.47929	0.92774	9.490100	1.748105	1.884261
75	19.73604	1.14772	226.51439	0.92121	9.577720	1.890263	2.051945
80	21.05178	1.15833	243.84938	0.91448	9.666278	2.034923	2.225219
85	22.36751	1.16906	261.48868	0.90757	9.755770	2.182123	2.404366
90	23.68325	1.17989	279.43670	0.90046	9.846197	2.331899	2.589690
95	24.99898	1.19084	297.69787	0.89314	9.937559	2.484289	2.781516
98	25.78843	1.19746	308.80672	0.88866	9.992825	2.576992	2.899877
100	26.31472	1.20190	316.27661	0.88562	10.029860	2.639328	2.980193

Sample Calculation

Assume that brine enters a cell at 50% saturation and leaves at 98% saturation. Determine the ratio of output volume to input volume.

Every gallon of 50% satruated brine entering the cell is composed of 0.95209 gallons of water and 1.20376 pounds of salt. If a gallon of fresh water was injected into the cell the resulting 98% saturated brine would contain 2.899877 pounds of salt per gallon of water. But since the actual brine entering the cell contains only 0.95209 gallons of water per gallon of brine, the weight of salt dissolved for every gallon of brine entering the cell is

$$0.95209 \frac{\text{gal water}}{\text{gal brine}} \times 2.899877 \frac{\text{lbs salt}}{\text{gal water}} = 2.76094 \frac{\text{lbs salt}}{\text{gal brine}}$$

Therefore the weight of salt dissolved in the cell per gallon of 50% saturated brine entering the cell is the difference in the salt content of the brine leaving the cell and the salt content of the brine entering the cell and is calculated as

$$2.76094 - 1.20376 = 1.55718 \frac{\text{lbs salt}}{\text{gal brine}}$$

The weight of salt dissolved converted to a volume dissolved is

$$1.55718 \text{ lbs salt} \times \frac{1}{134.838} \frac{\text{ft}^3}{\text{lbs salt}} \times 7.481 \frac{\text{gal}}{\text{ft}^3} = 0.086395 \text{ gal}$$

of new space created for every gallon of brine entering the cell.

The volume of 98% saturated brine produced by the dissolution process in the cell is

$$0.95209 \text{ gal water} \times \frac{1}{0.88866} \frac{\text{gal brine}}{\text{gal water}} = 1.071377 \text{ gal brine}$$

The volume of brine leaving the cell is therefore the volume of brine produced by the dissolution process minus the volume of space created and is calculated as

$$1.071377 - 0.086395 = 0.984982 \text{ gallons.}$$

Comparing the output and input volumes results in the following ratio

$$\frac{\text{Output Volume}}{\text{Input Volume}} = 0.984982$$

APPENDIX B

SOLUTION OF CUBIC EQUATION

The technique used to solve Equations 5-14a and 5-18a was taken from Newman (12) pages 197-9.

Equation 5-13 is rewritten symbolically as

$$Q_o^3 + a\,Q_o^2 + c = 0 \qquad \text{(B-1)}$$

where:

$$a = \frac{1.46022 \times 10^{-4}\, w_1}{1.353639572 \times 10^{-7}\, w_1}$$

$$= 1.078736194 \times 10^{3} \qquad \text{(B-2)}$$

$$c = -\frac{319.3415638\, w_2}{1.353639572 \times 10^{-7}\, w_1}$$

$$= -2.359132892 \times 10^{9}\,(w_2/w_1) \qquad \text{(B-3)}$$

Equation B-1 may be reduced by substitution of the following relationship:

$$Q_o = x - \frac{a}{3}. \qquad \text{(B-4)}$$

The reduced form is given by

$$x^3 + 3p\,x + 2q = 0. \qquad \text{(B-5)}$$

where:

$$p = -\frac{a^2}{9}$$

$$= 1\ 1.292968640 \times 10^{5} \qquad \text{(B-6)}$$

$$q = \frac{1}{2}\left(\frac{2}{27}a^3 + c\right)$$

$$= 4.649240234 \times 10^{7} - 1.179566446 \times 10^{9}\frac{w_2}{w_1} \qquad \text{(B-7)}$$

The classification of roots of Equation B-5 depends on the value of $q^2 + p^3$, or

$$q^2 + p^3 = \left(4.649240233 \times 10^{7} - 1.179566446 \times 10^{9}\frac{w_2}{w_1}\right)^2 + (-1.292968640 \times 10^{5})^3 \qquad \text{(B-8)}$$

For this equation the following situation occurs:

$$q^2 + p^3 > 0 \quad \text{for} \quad \frac{w_2}{w_1} < 2.371751149 \times 10^{-11} \qquad \text{(B-9a)}$$

$$q^2 + p^3 \leq 0 \quad \text{for} \quad 2.371751149 \times 10^{-11} \leq \frac{w_2}{w_1} < 7.88296454 \times 10^{-2} \qquad \text{(B-9b)}$$

$$q^2 + p^3 \geq 0 \quad \text{for} \quad 7.88296454 \times 10^{-2} \leq \frac{w_2}{w_1} \qquad \text{(B-9c)}$$

This research will be limited to values of w_2/w_1 being either zero or positive, so $q^2 + p^3$ can be negative, zero or positive as shown by Equation B-9.

For $q^2 + p^3 \geq 0$ the following solution known as Cardan's formula is used:

$$x = u + v, \tag{B-10}$$

where:

$$u = \sqrt[3]{-q + \sqrt{q^2 + p^3}} \tag{B-11}$$

$$v = \sqrt[3]{-q - \sqrt{q^2 + p^3}} \tag{B-12}$$

For $q^2 + p^3 \leq 0$ the following solution technique is given:

$$x_1 = 2\sqrt{-p}\ \cos\frac{\varphi}{3}, \tag{B-13a}$$

$$x_2 = -2\sqrt{-p}\ \cos\left(\frac{\varphi}{3} + 60^\circ\right) \tag{B-13b}$$

$$x_3 = -2\sqrt{-p}\ \cos\left(\frac{\varphi}{3} + 60^\circ\right) \tag{B-13c}$$

where:

$$\varphi = \cos^{-1}\frac{-q}{\sqrt{-p^3}} \text{ (in degrees)} \tag{B-14}$$

APPENDIX C

MANAGERIAL OPERATING RANGES FOR SUMP AND CAVERN CONSTRUCTION

TABLE X

MANAGERIAL OPERATING RANGE FOR SUMP CONSTRUCTION

$\frac{w_2}{w_1}$	k	Q_o	Managerial operating range	
			Q_{lower}	Q_{upper}
0.1	1.010	399	351	454
	1.020		333	478
	1.030		319	497
	1.040		308	512
	1.050		299	529
	1.060		291	543
	1.070		283	556
	1.080		277	568
	1.090		271	578
	1.100		265	591
0.5	1.010	794	702	895
	1.020		667	940
	1.030		641	975
	1.040		620	1006
	1.050		602	1033
	1.060		586	1059
	1.070		572	1083
	1.080		559	1105
	1.090		547	1126
	1.100		536	1147
1.0	1.010	1052	933	1183
	1.020		888	1240
	1.030		854	1286
	1.040		826	1325
	1.050		803	1361
	1.060		782	1393
	1.070		763	1423
	1.080		746	1452
	1.090		730	1479
	1.100		716	1505
2.0	1.010	1384	1231	1552
	1.020		1172	1625
	1.030		1128	1683
	1.040		1092	1733
	1.050		1062	1778
	1.060		1035	1820
	1.070		1010	1858
	1.080		988	1894
	1.090		968	1929
	1.100		949	1962

TABLE X (Continued)

$\frac{w_2}{w_1}$	k	Q_o	Managerial operating range	
			Q_{lower}	Q_{upper}
5.0	1.010	1968	1756	2199
	1.020		1673	2300
	1.030		1612	2379
	1.040		1563	2448
	1.050		1520	2509
	1.060		1482	2566
	1.070		1448	2618
	1.080		1417	2668
	1.090		1388	2715
	1.100		1362	2759
10.0	1.010	2550	2280	2843
	1.020		2175	2971
	1.030		2097	**
	1.040		2033	**
	1.050		1978	**
	1.060		1930	**
	1.070		1886	**
	1.080		1846	**
	1.090		1810	**
	1.100		1775	**

Values of Q_o, Q_{lower} and Q_{upper} are rounded off to the nearest whole number.

**Exceeds 3000 gpm.

TABLE XI

MANAGERIAL OPERATING RANGE FOR CAVERN INSTRUCTIONS

$\frac{w_2}{w_1}$	k	Q_o	Managerial operating range	
			Q_{lower}	Q_{upper}
0.1	1.010	494	442	551
	1.020		422	576
	1.030		407	595
	1.040		394	612
	1.050		384	627
	1.060		374	641
	1.070		366	653
	1.080		358	666
	1.090		351	677
	1.100		344	688
0.5	1.010	885	794	983
	1.020		759	1025
	1.030		733	1058
	1.040		711	1087
	1.050		692	1113
	1.060		676	1136
	1.070		661	1158
	1.080		648	1179
	1.090		635	1198
	1.100		623	1217
1.0	1.010	1130	1016	1254
	1.020		971	1307
	1.030		938	1349
	1.040		910	1385
	1.050		887	1418
	1.060		866	1447
	1.070		847	1475
	1.080		830	1500
	1.090		814	1525
	1.100		799	1548
2.0	1.010	1440	1256	1596
	1.020		1239	1663
	1.030		1197	1716
	1.040		1162	1761
	1.050		1132	1802
	1.060		1106	1839
	1.070		1082	1874
	1.080		1060	1906
	1.090		1040	1937
	1.100		1021	1966

TABLE XI (Continued)

$\frac{w_2}{w_1}$	k	Q_o	Managerial operating range	
			Q_{lower}	Q_{upper}
5.0	1.010	1977	1780	2188
	1.020		1703	2279
	1.030		1646	2351
	1.040		1599	2413
	1.050		1558	2468
	1.060		1522	2518
	1.070		1489	2565
	1.080		1460	2609
	1.090		1432	2650
	1.100		1407	2690
10.0	1.010	2507	2259	2773
	1.020		2162	2889
	1.030		2090	2979
	1.040		2030	**
	1.050		1979	**
	1.060		1933	**
	1.070		1892	**
	1.080		1855	**
	1.090		1820	**
	1.100		1787	**

Values of Q_o, Q_{lower} and Q_{upper} are rounded off to the nearest whole numbers.

**Exceeds 3000 gpm.

APPENDIX D

ALGORITHM TO DETERMINE OPTIMAL POLICY

An optimal policy is defined as 1) the produced brine flow rate that optimizes the research objective, and 2) an associated managerial operating range.

The following algorithm outlines the steps necessary to determine an optimal policy.

1. Describe the physical system. Assign numerical values to all system variables (pipe diameters, desired cavern size, depth to cavern roof, etc.) except the produced brine flow rate.
2. Establish an allowable range of investigation for the produced brine flow rate, and select a number of constant flow rates within this range. (This research was conducted using a total of ten constant flow rates, including the endpoints, equally spaced between 300 gpm and 3000 gpm.) Conduct simulated cavern construction activities to determine 1) total energy consumed and 2) construction time for each constant flow rate.
3. Plot data obtained in Step 2 and fit suitable equations to data.
4. Construct the mathematical value function reflecting the verbal research objective.
5. Determine the produced brine flow rate that optimizes the value function.

6. Perform a sensitivity analysis on the value function to determine how a deviation from the optimal flow rate affects the numerical value of the value function.
7. From the sensitivity analysis, determine the managerial operating range for the produced brine flow rate to maintain the numerical value of the value function within predetermined limits.

VITA

James Harry Norton

Candidate for the Degree of

Doctor of Philosophy

Thesis: OPTIMAL PROCEDURE FOR ENERGY MANAGEMENT IN SOLUTION MINING OF SALT DOME CAVERNS

Major Field: Industrial Engineering and Management

Biographical:

Personal Data: Born in Tulsa, Oklahoma, February 5, 1944, the son of Joseph Randolph Norton and Mildred Krueger Norton.

Education: Graduated from C. E. Donart High School, Stillwater, Oklahoma, in May, 1962; attended Oklahoma State University from June, 1962, until May, 1967; received Bachelor of Science degree in Mechanical Engineering from Oklahoma State University in May, 1967; received Master of Science degree from Oklahoma State University in May, 1971, with a major in Mechanical Engineering; completed requirements for the Doctor of Philosophy degree at Oklahoma State University in July, 1978.

Professional Experience: Project Engineer, Aluminum Company of America, June, 1967, until August, 1969; Engineer, Fenix & Scisson, Incorporated, part time basis at various times from 1963 until 1974, full time basis since 1974; Registered Professional Engineer in the state of Oklahoma.